The Pennsylvania State University
The Graduate School

GROWTH RATE OF PERIODIC ORBITS FOR GEODESIC FLOWS ON SURFACES WITH REGIONS OF POSITIVE CURVATURE

A Dissertation in
Mathematics
by
Bryce Weaver

Submitted in Partial Fulfillment
of the Requirements
for the Degree of

Doctor of Philosophy

August 2008

The dissertation of Bryce Weaver was reviewed and approved* by the following:

Anatole Katok
Professor of Mathematics
Dissertation Advisor, Chair of Committee

Yakov Pesin
Professor of Mathematics

Omri Sarig
Professor of Mathematics

David Abler
Professor of Agricultural, Environmental &
Regional Economics and Demography

John Roe
Head of the Department of Mathematics

*Signatures are on file in the Graduate School.

Abstract

We construct a Margulis measure on the unit tangent bundle of compact surfaces that have regions of positive curvature. This measure is then used to obtain a lower bound Cèsaro estimate on $P_\epsilon(t)$, which is the number of periodic orbits of period $t \pm \epsilon$ for the geodesic flow. This is the first step toward obtaining precise asymptotics and suggests that $P_\epsilon(t)$ grows like $\frac{e^{kt}}{t}$, for some constant k.

Table of Contents

List of Figures **vi**

Acknowledgments **vii**

Chapter 1
Introduction and History **1**
1.1 Overview 1
1.2 History 2
1.3 Hyperbolic flows and the Margulis Construction 3
1.4 Non-uniform Hyperbolic flows and Invariant Cone Families 4
1.5 The Differential of Geodesic Flows and the Sasaki Metric 5

Chapter 2
The Geodesic Flows on Special Surfaces **7**
2.1 The Cones and Caps 7
2.2 Qualitative Behavior of the Differential in the Caps 10
2.3 Explicit Formulas for the Jacobi Fields 14
2.4 Relation of Values to the Entry Angle 18
2.5 Essential Properties of the Flow 26
2.6 Proof of Lemma 3.4.4 in Local Coordinates 31

Chapter 3
Existence and Properties of Unstable and Weak-Unstable Manifolds **35**
3.1 Basic Setup, Notations, and Properties 35
3.2 Existence and Uniqueness of Local and Global Unstable Manifolds . 38

3.3 Some Properties of Unstable Manifolds 45
3.4 Behavior Near the Singular Set 48
3.5 Behavior Under Holonomy Maps 51

Chapter 4
Long Term Behavior on Unstable Manifolds **56**
4.1 Comparative Growth Rate of Unstable Manifolds 56
4.2 Long Term Behavior of Holonomy Equivalents 60
4.3 Translating to Functions 64

Chapter 5
Construction of Conditional Measures **68**
5.1 Special Linear Functionals 68
5.2 Finding Conditional Measure on Unstable Manifolds 72
5.3 Holonomy Invariance and Other Properties 74

Chapter 6
Construction of Margulis Measure **80**
6.1 From Flow Box to the Manifold 80
6.2 Properties of the Measure 82

Chapter 7
Counting of Periodic Orbits **84**
7.1 Finding Closed Orbits 84
7.2 Main Result 86
7.3 Further Work 87

Appendix A
Geometric Computations **88**
A.1 Horizontal and Vertical Subspaces in Local Coordinates 88
A.2 Horizontal and Vertical Subspaces in Local Coordinates for the Unit Tangent Bundle of Surfaces 90
A.3 The Differential on the Orthogonal Space for Geodesic Flows on Surfaces 93

Bibliography **95**

List of Figures

2.4.1 Over and underestimation of the integral of the curvature. 20
2.5.1 Splitting of U near orbits in N. 29

3.2.1 The generated weak-stables would open like a book. 41
3.4.1 The local unstable approaches a double copy. 50
3.5.1 The time distance is $|t_1 - t_2|$. 52
3.5.2 The holonomy image of a local weak-unstable. 54

4.1.1 The tiling and its weak-stable image. 58

5.3.1 A flow box. 77

7.1.1 A closed orbit in each full component of intersection. 85

Acknowledgments

I would like to thank: my advisor, Professor Anatole Katok, for putting me on the right track, my committee members, Professor Omri Sarig, Professor Yakov Pesin, and Professor David Abler, for their guidance, and Professor Patrick Eberlein for his assistance. Thank you France for your belief in me.

Chapter 1

Introduction and History

1.1 Overview

We establish a verifiable list of properties displayed by a class of non-uniformly hyperbolic geodesic flows on surfaces. This list of properties combined with local analysis is sufficient to construct a Margulis-measure. This measure is used to generate estimates on the number of periodic orbits of an approximate length. The primary property of interest is the invariance of cones. This work could be considered as a blueprint for estimating the growth rate of periodic orbits on similar classes of system.

The chapters split into three major parts.

1. In Chapter 2, we look at the class of examples and establish the properties of the flow.

2. In Chapters 3 and 4, we take the properties established in Chapter 2 and explore their consequences. Namely, how these properties allow us to have some of the structure displayed by hyberbolic systems.

3. In Chapters 5 to 7, we adapt the work of G. Margulis to the particular class of systems that we are considering. After developing simple properties of our Margulis-measure, such as ergodicity, we obtain the main result.

The reader more interested in the analytic constructions than the development of properties could begin with Chapter 3.

1.2 History

This dissertation has basically two histories. The first one is the history of related results on the asymptotics of the number of the periodic orbits. The second one is that of the class of examples used.

In his 1970 thesis, G. Margulis obtains precise asymptotics for the growth rate of periodic orbits for the class of uniformly hyperbolic flows. For a topologically mixing flow, ϕ_t, on a compact Riemannian manifold, the number of periodic orbits of period less than or equal to t satisfies

$$\lim_{t\to\infty} thP(t)e^{-th} = 1, \tag{1.1}$$

where h is the topological entropy of the flow, see [HK]. It is both this result and this technique, which inspired the present work.

The main related results in the class of non-uniformly hyperbolic theory is for rank 1, non-positive curvature geodesic flows. For $P_{\text{reg}}(t)$ the number of regular periodic orbits of period less than t, we have a result from G. Knieper that there exists a constant $C > 1$ such that for t sufficiently large,

$$\frac{1}{C} \leq thP_{\text{reg}}(t)e^{-th} \leq C.$$

Later R. Gunesch, in his thesis (see [Gu]), improves this result to precise asymptotics of the form given by Margulis. Since the underlying techniques are different than what we are interested in, we do not dwell on them here. However for the interested reader, some of the work of G. Knieper including the result given above can be found in [GK]. A nearly comprehensive development of manifolds of non-positive curvature can be found in [Eb].

In the 1980's, this class of metrics was developed to build geodesic flows on the unit tangent bundle of S^2 that are ergodic with respect to volume. The main tool is the development of the focusing cap by V. Donnay. He shows that surfaces who have negative curvature outside of focusing caps are ergodic, see [VD1] and [VD2]. We return to the discussion of focusing caps in Chapter 2. Later, K. Burns and M. Gerber show, with some slight restrictions, that these flows are Bernoulli with respect to volume, see [BG]. It is the analysis from their paper that is the starting

point for the development of properties for the present work.

1.3 Hyperbolic flows and the Margulis Construction

A complete development of the Margulis construction can be found in [HK] and [Ma]. Here, the goal is to give some of the basic concepts.

Let ϕ_t be a differentiable flow on a compact Riemannian manifold M without fixed points (the definition works for invariant subsets). The flow is *Anosov* or *Hyberbolic* if at every $x \in M$, the tangent space can be decomposed into the direct sum of three continuously varying subspaces [the unstable space $E^u(x)$, the stable space $E^s(x)$, and the subspace corresponding to the direction of flow $X(x)$] satisfying the following properties:

1. the spaces are invariant under the action of the differential, and
2. there exist positive constants a, b, c such that for $\xi \in E^u(x)$, $\eta \in E^s(x)$, and $t \geq 0$

$$\begin{aligned} |D\phi_t \xi| &\geq a\,|\xi|\,e^{ct} && (1.2)\\ |D\phi_{-t} \xi| &\leq b\,|\xi|\,e^{-ct} && (1.3)\\ |D\phi_{-t} \eta| &\geq a\,|\eta|\,e^{ct} && (1.4)\\ |D\phi_t \eta| &\leq b\,|\eta|\,e^{-ct}. && (1.5) \end{aligned}$$

It is well understood that under these conditions the spaces E^u, E^s, $E^u \oplus X$, and $E^s \oplus X$ are uniquely integrable and foliate the space. They are referred to as the *unstable manifolds*, *stable manifolds*, *weak-unstable manifolds*, and *weak-stable manifolds* respectively. In our setting, we construct similarly named objects that have related properties.

The work of G. Margulis involves constructing conditional measures on the weak-unstable manifolds (respectively the weak-stable manifolds) that expand at a uniform exponential rate (respectively decays). The conditional measures are found as a fixed point under an action of the flow on a class of special linear

operators. The major required estimate is that the long term volume of any two sets in the weak-unstable manifolds is of the same order of magnitude (the role of which is played by Corollary 4.1.1 in this work).

A measure is then constructed by integrating the conditional measures locally. The technical difficulty is showing that this procedure is well defined. This is overcome by showing that the long term ratio of holonomy equivalent sets in the weak-unstable manifolds goes to one (the role of which is played by Lemma 4.2.1). After developing several properties of the measure, namely invariance and mixing, the number of periodic orbits are estimated by examining the way that the image of a *flow box* (a box constructed from attaching local pieces of stable manifolds to a local piece of weak-unstable manifold) intersects the flow box itself, see Figure 7.1.1. Mixing has not yet been shown in the present work and is replaced by ergodicity (Theorem 6.2.1). This is the largest difference between result of Equation 1.1 and our present result of Theorem 7.2.1.

1.4 Non-uniform Hyperbolic flows and Invariant Cone Families

The field of non-uniform hyperbolic systems is exceedingly rich. Although we do not use the major results directly from the field, our systems here fall under this category. An excellent coverage can be found in [BP]. For a thorough examination of the relationship between invariant cones and positive Lyapunov exponents (a condition for non-uniform hyperbolicity), one can see [BK].

There is a lot of knowledge on the existence of unstable and stable manifolds for flows on non-uniform hyperbolic sets. However, typical results are based on a pre-existing measure. Since we seek to construct a measure that is singular with respect to the pre-existing measure, we do not directly use these results.

1.5 The Differential of Geodesic Flows and the Sasaki Metric

This section consists of excerpts pulled directly from [GK]. A basic background in Riemannian geometry can be found in [DC2]. The structure presented here, is used in Chapter 2; particularly the relationship between the differential of a geodesic flow on unit tangent bundle and solutions to the Jacobi equations.

Let $\tilde{M}, \langle \cdot, \cdot \rangle$, be a smooth Riemannian manifold, $T\tilde{M}$ be its tangent bundle, and $\pi : T\tilde{M} \to \tilde{M}$ be the canonical projection. Consider $TT\tilde{M}$, the tangent bundle of $T\tilde{M}$. For $v \in T\tilde{M}$, we have two natural linear maps from $T_vT\tilde{M}$ into $T_{\pi v}\tilde{M}$. The first map comes from the canonical projection π and is given by $d\pi_v : T_vT\tilde{M} \to T_{\pi v}\tilde{M}$. The second map comes from the Levi-Civita connection D. Let a vector in $\xi \in T_vTM$ be given by $\xi = \left.\frac{d}{ds}\right|_{s=0} X(s)$ for $X(s) : (-\epsilon, \epsilon) \to T\tilde{M}$ a smooth curve with $X(0) = v$. Furthermore, let $\gamma(s) = \pi \circ X(s)$ be the projection of the curve in $\tilde{M}$ and $\frac{D}{ds}$ the covariant derivative along the curve. We define the connection map, $C_v : T_vT\tilde{M} \to T_{\pi v}\tilde{M}$ to be

$$C_v(\xi) = C_v\left(\left.\frac{d}{ds}\right|_{s=0} X(s)\right) = \left.\frac{D}{ds}\right|_{s=0} X(s).$$

From these two linear maps, we generate the linear map $(d\pi_v, C_v) : T_vT\tilde{M} \to T_{\pi v}\tilde{M} \times T_{\pi v}\tilde{M}$ by $\xi \to (d\pi_v\xi, C_v\xi)$. This is a linear isomorphism. We let the *Horizontal space* be the one that corresponds to

$$\left\{(w, 0) \,\middle|\, w \in T_{\pi v}\tilde{M}\right\}$$

and the *vertical space* be the one that corresponds to

$$\left\{(0, w) \,\middle|\, w \in T_{\pi v}\tilde{M}\right\}.$$

For the linear maps, $d\pi_v$, C_v, and the horizontal and vertical spaces in local coordinates, see Appendix A.1.

There are several major uses of the decomposition of the tangent space into horizontal and vertical spaces.

1. We can define a natural Riemannian metric $\langle \cdot, \cdot \rangle_S$ on $T\tilde{M}$, called the *Sasaki Metric*. For two vectors ξ and η in T_vTM

$$\langle \xi, \eta \rangle_S := \langle d\pi_v \xi, d\pi_v \eta \rangle + \langle C_v \xi, C_v \eta \rangle . \tag{1.6}$$

2. The generating vector field for the geodesic flow on $T\tilde{M}$ at $v \in TM$ is given by the vector $(v, 0) \in T_{\pi v}\tilde{M} \times T_{\pi v}\tilde{M}$.

3. We obtain a characterization of the differential via Jacobi fields. Let $\xi = (\xi_h, \xi_v)$ be the decomposed form of a vector in $T_vT\tilde{M} \backsim T\tilde{M} \times T\tilde{M}$, ϕ_t the geodesic flow, and $D\phi_t$ its differential. Furthermore, let $\dot{}$ denote $\dfrac{D}{dt}$, the covariant derivative along the curve $\gamma(t) = \pi(\phi_t v)$, and J the solution to the Jacobi equation[1]

$$\ddot{J} + R(\phi_t(v), J(t))\phi_t(v) = 0, \tag{1.7}$$

   where R is the curvature tensor. Then, the decomposed form of $D\phi_t\xi$ is given by

$$D\phi_t(\xi_h, \xi_v) = \left(J(t), \dot{J}(t)\right), \tag{1.8}$$

   where J has initial condition $J(0) = \xi_h$ and $\dot{J}(0) = \xi_v$.

4. For $v \in SM$, the unit tangent bundle, we have an elegant way of describing $T_vS\tilde{M}$ and $T_v^{\perp}S\tilde{M}$, the subspace perpendicular to the flow direction. They are

$$T_vS\tilde{M} = \left\{(\xi_h, \xi_v) \in T_vT\tilde{M} : \xi_v \perp v\right\} \tag{1.9}$$

   and consequently,

$$T_v^{\perp}S\tilde{M} = \left\{(\xi_h, \xi_v) \in T_v^{\perp}T\tilde{M} : \xi_h \perp v\right\}. \tag{1.10}$$

[1] We use the definition of the curvature tensor as in [DC2].

Chapter 2

The Geodesic Flows on Special Surfaces

In this chapter, we discuss the flows and develop the properties that we need for Chapters 3 - 7. It is distinct in its nature from the other chapters in that here we consider our flow as a geodesic flow on the unit tangent bundle of a compact Riemannian surface. In the following chapters, the flow is morally viewed as a differentiable flow on a compact 3-dimensional Riemannian manifold that satisfies the properties established for these geodesic flows.

Most of this chapter is devoted to tools that are intended for internal consumption only and hence have notations that would be too cumbersome to use elsewhere. In particular, we work mostly in a particular local parametrization, which is not done anywhere else. The only sections that contain material quoted directly by other chapters are the first part of Section 2.1, Section 2.5, and Proposition 2.6.1 from Section 2.6. Section 2.6 is a proof of a lemma that, in a chronological sense, belongs in Chapter 3. However, the proof uses tools and notation particular to this chapter and is included here.

2.1 The Cones and Caps

We define the flow that we consider throughout this document. We also define the cones, the open set where they are defined, and their most basic properties. We finish with explicit formulation of the caps in local coordinates. This formulation

is useful in developing the properties of the system that interest us. The first part of this section is used in the subsequent chapters, but the explicit formulations are used uniquely here.

Consider a surface $\tilde{M}$ with a C^3 metric $\langle \cdot, \cdot \rangle_{\tilde{M}}$ that has negative curvature everywhere except in focusing caps. These caps are given as surfaces of revolution where the negative curvature is divided from the positive curvature by a closed geodesic where the curvature is evidently zero. We give more details of the caps below. For a discussion of these caps see either [BG], who gives a property guarantying that a cap is focusing, or [VD1].

The flow, ϕ_t, is the geodesic flow on the unit tangent bundle $M = S\tilde{M}$ given the Sasaki metric. For a discussion on the Sasaki metric and some of the following setup see for example [GK] or Section 1.5. Let $U \subset S\tilde{M}$ be the open set of elements that have footprints in the region of negative curvature. The cones are contained in the invariant planes, $T_x^{\perp} S\tilde{M}$, the plane orthogonal to the flow direction at $x \in S\tilde{M}$. The cones are given for all $x \in U$ by

$$C(x) = \left\{ V \in T_x^{\perp} S\tilde{M} | \, \langle V_h, V_v \rangle_{\tilde{M}} \geq 0 \right\}$$

where V_h and V_v are the horizontal and vertical components of V. These are the cones that are invariant in the setting of non-positive curvature. The complement cones, $\widehat{C}(x)$, are the closure of the complement of $C(x)$ in the orthogonal plane and are explicitly given by

$$\widehat{C}(x) = \left\{ V \in T_x^{\perp} S\tilde{M} | \, \langle V_h, V_v \rangle_{\tilde{M}} \leq 0 \right\}.$$

By symmetry of the geodesic flow, these cones will have the same behavior for negative times as $C(x)$ do for positive times. As a result, we typically prove properties only for one and use it for the other.

From Appendix A.3, for $V \in T_x^{\perp} S\tilde{M}$, we can represent $D\phi_t \left(V_h, V_v \right)$ by $\left(J(t), \dot{J}(t) \right)$ where J is the solution of the equation

$$\ddot{J}(t) + \kappa(t) J(t) \;\; = \;\; 0 \tag{2.1}$$

with initial conditions $\left(J(0), \dot{J}(0) \right) = (V_h, V_v)$. The $\kappa(t) = \kappa \left(\gamma_x(t) \right)$ is the curva-

ture of $\tilde{M}$ at $\gamma_x(t)$ where γ_x is the geodesic in $\tilde{M}$ with initial condition x. The orthogonal direction is one dimensional. Consequently, we can view solutions to Equation 2.1 as either a vector field along the geodesic or a scalar value.

The cones, from standard theory of non-positive curvature, are invariant as long as $\phi_t(x)$ does not leave U. Outside of U, we do not define any cones. The focusing caps are precisely those which preserve these cones on returns to U. Much of the work analyzes more precisely what occurs in these caps. Our caps will be a subset of the full set of focusing caps, including those described in [BG].

Let the cap be a surface of revolution given by

$$F(u, v) = (f(v)\cos u, f(v)\sin u, g(v))$$

with $u \in S^1$ and $v \in (-\delta, L]$ where $\delta, L > 0$ and $\lim_{v\to L} f(v) = 0$. For the properties that we want, assume the following conditions:

1. $((f'(v))^2 + (g'(v))^2 = 1$ and $f(v) > 0$ to simplify calculations,
2. $f'(0) = f''(0) = 0$ to separate regions of positive and negative curvature by a closed geodesic where the curvature is zero,
3. $f''(v) < 0$ for $v > 0$ and $f''(v) > 0$ for $v < 0$ to give the surface negative curvature for $v < 0$ and to give the surface positive curvature for $v > 0$,
4. there exists an odd integer $k \geq 3$ such that f is C^k and $f^k(0) < 0$.

One should note a few items. The curve given by $v = 0$ maps out a closed geodesic with curvature 0 along it. Any curve that enters the region where $v > 0$ will leave the cap altogether. Finally, the coordinate v represents the distance of the point from this closed geodesic.

The first condition is standard and allows us to immediately calculate the local representation of our metric, the Christoffel symbols, and the curvature of the surface in the cap, see for example [DC1]. We have the local representation

$$g_{11}(u, v) = f^2(v),$$

$$g_{12}(u, v) = g_{21}(u, v) = 0,$$

and

$$g_{22}(u,v) = 1.$$

Our connection coefficients are

$$\Gamma^2_{11} = -f'(v)f(v),$$

$$\Gamma^1_{12} = \Gamma^1_{21} = \frac{f'(v)}{f(v)},$$

and

$$\Gamma^1_{11} = \Gamma^2_{12} = \Gamma^2_{21} = \Gamma^1_{22} = \Gamma^2_{22} = 0.$$

Equivalently, we have

$$\begin{aligned}
\nabla_{\frac{\partial}{\partial u}} \frac{\partial}{\partial u} &= -f'(v)f(v)\frac{\partial}{\partial v}, \\
\nabla_{\frac{\partial}{\partial u}} \frac{\partial}{\partial v} &= \nabla_{\frac{\partial}{\partial v}} \frac{\partial}{\partial u} = \frac{f'(v)}{f(v)}\frac{\partial}{\partial u}, \text{ and} \\
\nabla_{\frac{\partial}{\partial v}} \frac{\partial}{\partial v} &= 0.
\end{aligned}$$

Finally, the curvature is given by

$$\kappa(u,v) = -\frac{f''(v)}{f(v)}. \tag{2.2}$$

2.2 Qualitative Behavior of the Differential in the Caps

Before going into a more computative analysis of the Jacobi fields, we make use of some tools constructed in [BG], in particular the Jacobi fields that correspond to S and C. The C here is to be consistent with the notation used by K. Burns and M. Gerber and should not be confused with the cones, $C(x)$, from the previous section. Their tools and notation are used exclusively in this section, and only the consequences are used elsewhere. The term qualitative does not mean that these results are purely qualitative, but is used to distinguish them from the much more computational results of the subsequent sections.

Most of the properties that we seek for the overall construction are obvious both outside of the cap and for orbits that do not come close to the closed geodesics separating the regions of negative and positive curvature. Notice that each of these closed geodesics corresponds to two closed orbits of the flow with opposite directions. By symmetry, the behavior only differs by orientation in neighborhoods of these two orbits. Thus, we examine the orbits that enter the positive curvature region close to one of these orbits. We will call the angle formed between the geodesic given and the parallel at $v = 0$ the *entry angle*, α. This is expanded to a natural local coordinate system for the unit tangent bundle in the next section.

Let γ_α be a geodesic that has entry angle $0 < \alpha < \frac{\pi}{2}$. By symmetry, the u value does not matter; all such geodesics have the same form. They move until they achieve the maximum v-value, $v_{\max} = v_{\max}(\alpha)$, and then return (again by symmetry) on a curve that is a reflection of the original. We call this point the *turning point*. Let T_0 be the length of γ_α from the entry to turning point and parameterize γ_α on $[-T_0, T_0]$ so that $v\left(\gamma_\alpha\left(-T_0\right)\right) = v\left(\gamma_\alpha\left(T_0\right)\right) = 0$ and consequently $v\left(\gamma_\alpha\left(0\right)\right) = v_{\max}$.

By the parametrization $\kappa(t) = \kappa\left(\gamma_\alpha(t)\right)$, the curvature of the surface at the point of $\gamma_\alpha(t)$, is even. Construct the Jacobi fields S and C with initial conditions $S(0) = 0$, $\dot{S}(0) = 1$, $C(0) = 1$, and $\dot{C}(0) = 0$. These are the values at the turning points. Note that S corresponds to a scalar multiple of the orthogonal projection of the Jacobi field given by rotation in the u direction, see [BG]. We also see this by explicit formulation in the next section (it is a scalar multiple of H, see page 17). Hence at $\pm T_0$, we have $\dot{S}(\pm T_0) = 0$. Clearly S and $\dot{C}$ are odd functions, and $\dot{S}$ and C are even.

Lemma 2.2.1. *A cap is focusing if and only if $C(-T_0) \leq 0$ for all angles α.*

Proof: By preservation of the symplectic form,

$$C(-T_0)\dot{S}(-T_0) - S(-T_0)\dot{C}(-T_0) = C(0)\dot{S}(0) - S(0)\dot{C}(0) = 1,$$

and as $\dot{S}(-T_0) = 0$, and $S(-T_0) < 0$, we have

$$\dot{C}(-T_0) = \frac{-1}{S(-T_0)} > 0.$$

Let J be a solution to the Jacobi equation with

$$J\left(-T_0\right)\dot{J}\left(-T_0\right) \geq 0.$$

Without loss of generality, assume that both $J\left(-T_0\right)$ and $\dot{J}\left(-T_0\right)$ are greater than or equal to 0. Then $J(t) = AC(t) + BS(t)$ with $A \geq 0$ and $B \leq \dfrac{AC\left(-T_0\right)}{S(-T_0)}$. By the properties of C and S, we have

$$J(T_0) = AC(-T_0) - BS(-T_0) \leq 0$$

and $\dot{J}(T_0) = -AC(-T_0) \leq 0$, hence the cap is focusing.

For the other sense, we prove the contrapositive. Assume that $C(-T_0) > 0$. For J with initial conditions $J(-T_0) = 0$ and $\dot{J}(-T_0) = 1$, we have

$$J(t) = \frac{1}{\dot{C}(-T_0)}C(t) - \frac{C(-T_0)}{S(-T_0)\dot{C}(-T_0)}S(t).$$

By these properties, $J(T_0) = 2\dfrac{C(-T_0)}{\dot{C}(-T_0)} > 0$ and $\dot{J}(T_0) = -1$. Hence, the cap is not focusing. $\Diamond$

From the previous lemma, we also obtain a lemma demonstrating that passing through the region $v \geq 0$ of the cap results in growth (or at least not a decrease in size) for the vectors in our cones. Although this result is obvious, it is the beginning tool that will show us that unstable vectors grow and stable vectors do not.

Corollary 2.2.1. *If the cap is a focusing cap, and* $J\left(-T_0\right)\dot{J}\left(-T_0\right) \geq 0$ *then*

$$\left\|\left(J\left(T_0\right), \dot{J}\left(T_0\right)\right)\right\| \geq \left\|\left(J\left(-T_0\right), \dot{J}\left(-T_0\right)\right)\right\|.$$

Proof: Use the proof above. $\Diamond$

Let us consider a related profile to the profile of $\left\|\left(J(t), \dot{J}(t)\right)\right\|$:

$$\left\|\left(J(t), \dot{J}(t)\right)\right\|^2 = J^2(t) + \dot{J}^2(t).$$

We are interested in finding and controlling the maximums and minimums of vec-

tors under the differential. By analyzing this equation, we are able to isolate them. The derivative yields:

$$\begin{aligned}\frac{d\left(\left\|\left(J(t),\dot{J}(t)\right)\right\|^2\right)}{dt} &= 2\left(J\dot{J}+\dot{J}\ddot{J}\right)\\ &= 2J\dot{J}\left(1-\kappa(t)\right).\end{aligned}$$

For $\kappa(t) < 1$, this has critical points precisely when $J = 0$ or $\dot{J} = 0$. Taking a second derivative, when $J = 0$ (and consequently $\dot{J} \neq 0$ for nontrivial vectors), gives

$$\left.\frac{d^2\left(\left\|\left(J(t),\dot{J}(t)\right)\right\|^2\right)}{dt^2}\right|_{J=0} = 2(\dot{J})^2\left(1-\kappa(t)\right) > 0.$$

Therefore, this is a local minimum for the norm of $\left(J(t),\dot{J}(t)\right)$. Furthermore, if we assume that $\kappa(t) > 0$, the second derivative at $\dot{J} = 0$ is

$$\left.\frac{d^2\left(\left\|\left(J(t),\dot{J}(t)\right)\right\|^2\right)}{dt^2}\right|_{\dot{J}=0} = 2J\ddot{J}\left(1-\kappa(t)\right) = -2\kappa(t)J^2\left(1-\kappa(t)\right) < 0$$

making this point a local maximum.

We can consider entry angles small enough so that the curvature remains less than 1 along the geodesic. For Jacobi fields that start with $\left(J\left(-T_0\right),\dot{J}\left(-T_0\right)\right)$ in the first quadrant, the following becomes evident.

Lemma 2.2.2. *If a cap is focusing and* $J\left(-T_0\right)\dot{J}\left(-T_0\right) \geq 0$ *then*

$$\max\left\{\left\|\left(J(t),\dot{J}(t)\right)\right\|\right\}$$

is either achieved in $-T_0 \leq t \leq 0$*, or at* $t = T_0$*, for all* α *sufficiently small.*

Proof: Without loss of generality, assume that $\left(J\left(-T_0\right),\dot{J}\left(-T_0\right)\right)$ is in the first quadrant. By the discussion above, we know that the local maximum occurs at the points where $\dot{J}(t) = 0$. If $J(t)$ is a multiple of $S(t)$, the maximum occurs at $\pm T_0$. Assume that $\dot{J}(-T_0) > 0$: in this case the profile starts in the first quadrant,

moves to the the fourth quadrant, before $t = 0$, the moves into and finishes in the third quadrant. By our work above, this implies that $\left\| \left(J(t), \dot{J}(t) \right) \right\|$ has a profile of increasing, then decreasing through the turn before increasing to the end. Consequently, the maximum either occurs at the local maximum before the turn or at T_0. $\Diamond$

2.3 Explicit Formulas for the Jacobi Fields

In this section, we give a parametrization of the unit tangent bundle of the caps. This parametrization is used to convert the Jacobi equation into a second order ordinary differential equation (ODE) in local coordinates. Because a pre-existing solution is known, we are able to generate a basis for the set of solutions through basic ODE theory. The explicit formulas are given at the end of the section and will be used to generate the results that require real computational knowledge of the Jacobi fields. Throughout this section, we assume that the entry angles α, and consequently the coordinate θ, are small. Namely, we need that $-\frac{\pi}{2} < \theta < \frac{\pi}{2}$ and that the curvature remains less than one.

In order to understand the differential of the geodesic flow, $D\phi_t$, on the unit tangent bundle in the cap, $\mathcal{C}$, let us parameterize $S\mathcal{C}$ by (u, v, θ). θ is the angle that $X \in S_{(u,v)}\mathcal{C}$ forms with the tangent of the parallels, $\frac{\partial}{\partial u}$, measured clockwise. Restated, (u, v, θ) is associated with

$$\left(u, v, \frac{\cos\theta}{f(v)} \frac{\partial}{\partial u} + \sin\theta \frac{\partial}{\partial v} \right) \in S\mathcal{C}.$$

This gives unit length vectors in the tangent bundle by the local representation presented on page 9.

From the Appendix A.2, we see that in our local coordinates:

$$\frac{\partial}{\partial \theta} \tag{2.3}$$

is a unit length vector in the vertical direction,

$$\frac{\cos\theta}{f(v)} \frac{\partial}{\partial u} + \sin\theta \frac{\partial}{\partial v} + \frac{\cos\theta f'(v)}{f(v)} \frac{\partial}{\partial \theta} \tag{2.4}$$

is the unit length vector field that gives the flow, and

$$-\frac{\sin\theta}{f(v)}\frac{\partial}{\partial u}+\cos\theta\frac{\partial}{\partial v}-\frac{\sin\theta f'(v)}{f(v)}\frac{\partial}{\partial\theta} \tag{2.5}$$

is the unit length vector field in the horizontal direction orthogonal to the flow direction and consistent with the orientation given by $\dfrac{\partial}{\partial\theta}$ on the underlying space.

We develop precise formulae for the solutions to the Jacobi fields in the cap. Naturally, for an orbit of the geodesic flow, we have a parametrization $u(t)$, $v(t)$, and $\theta(t)$ in these coordinates.

Now let us consider orbits that enter the positive curvature part with entry angle α. Note that this is the value of the coordinate θ when $v=0$. When the flow is in the surface of revolution, the v is a function of t. However, if we consider only the part of the curve before the turning point, we can view t as a function of v. Parameterizing against v and letting $\theta=\theta(v)$ for a given entry angle α, we have

$$\frac{dv}{dt}=\sin\theta.$$

We can view $J(t)$ as a function of v, namely $J(t(v))$. Letting $'$ represent differentiation with respect to v, we establish a differential equation for J in terms of v.

Using *Clairaut's relation*

$$f(v)\cos\theta = \text{ constant } = f(0)\cos\alpha, \tag{2.6}$$

we see, via the implicit function theorem, that

$$\frac{\partial\theta}{\partial v}=\frac{f'(v)\cos\theta}{f(v)\sin\theta}.$$

We have

$$\frac{dJ}{dt}(v)=\frac{dv}{dt}J'(v)=\sin\theta J'(v).$$

Taking the second derivative gives

$$\frac{d^2J}{dt^2}(v) \;=\; \frac{d}{dt}\left(\sin\theta J'(v)\right)$$

$$\begin{aligned} &= \frac{dv}{dt}\frac{d\theta}{dv}\left(\cos\theta J'(v)\right) + \sin\theta\frac{dv}{dt}J''(v) \\ &= \sin\theta\frac{f'(v)\cos\theta}{f(v)\sin\theta}\left(\cos\theta J'(v)\right) + \sin^2\theta J''(v) \\ &= \frac{f'(v)\cos^2\theta}{f(v)}J'(v) + \sin^2\theta J''(v). \end{aligned}$$

Plugging these into the differential Equation 2.1, we have

$$\begin{aligned} 0 &= \frac{d^2J}{dt^2}(v) + \kappa(v)J(v) \\ &= \sin^2\theta J''(v) + \frac{f'(v)\cos^2\theta}{f(v)}J'(v) - \frac{f''(v)}{f(v)}J(v), \end{aligned}$$

or

$$J''(v) + \overbrace{\cot^2\theta\frac{f'(v)}{f(v)}}^{p(v)}J'(v) - \csc^2\theta\frac{f''(v)}{f(v)}J(v) = 0. \tag{2.7}$$

In order to develop a spanning set of solutions to this differential equation, we notice that we already have one solution, namely the projection of $-\dfrac{\partial}{\partial u}$ onto the orthogonal space;

$$h(v) = \sin\theta f(v). \tag{2.8}$$

The procedure for finding a linearly independent solution is a straightforward reduction of order, see for example [BDP]. The key term is $p(v)$, marked in Equation 2.7;

$$p(v) = \frac{\cos\theta}{\sin\theta}\frac{\cos\theta f'(v)}{\sin\theta f(v)} = \frac{(\sin\theta)'}{\sin\theta}.$$

This immediately gives us

$$\exp\left(-\int p(s)ds\right) = \frac{1}{\sin\theta}.$$

We can now derive an explicit formula for a second solution to the differential

equation:

$$q(v) = h(v) \int_0^v \frac{1}{h^2(s)\sin\theta} ds. \tag{2.9}$$

Calculating directly, we have

$$\begin{aligned} \frac{d}{dt}h(v) &= \sin\theta\ h'(v) \\ &= \sin\theta\ \left(\cos\theta \left(\frac{\cos\theta f'(v)}{\sin\theta f(v)}\right) f(v) + \sin\theta\ f'(v)\right) \\ &= f'(v). \end{aligned}$$

Hence,

$$\begin{aligned} \frac{d}{dt}q(v) &= \left(\frac{1}{h(v)} + f'(v)\int_0^v \frac{1}{h^2(s)\sin\theta} ds\right) \\ &= \frac{1}{h(v)}\left(1 + f'(v)q(v)\right). \end{aligned}$$

This gives us a pair of vector fields that tell us how $D\phi_t$ maps the tangent space orthogonal to the flow. It is a linear combination of

$$H(v) = \left(h(v), f'(v)\right), \text{ and} \tag{2.10}$$

$$Q(v) = \left(q(v), \frac{1}{h(v)}\left(1 + f'(v)q(v)\right)\right), \tag{2.11}$$

which have initial conditions at $v = 0$ of

$$\begin{aligned} H(0) &= \left(f(0)\sin\alpha, 0\right), \text{ and} \\ Q(0) &= \left(0, \frac{1}{f(0)\sin\alpha}\right), \end{aligned}$$

respectively. Analyzing Equations 2.10 and 2.11 is one of the primary tools in most of our computations.

Using the equations for horizontal and vertical spaces (Equations 2.5 and 2.3), we can give H as function of v and θ

$$H\left(v,\theta\right) = \sin\theta f(v)\left(-\frac{\sin\theta}{f(v)}\frac{\partial}{\partial u} + \cos\theta\frac{\partial}{\partial v} - \frac{\sin\theta f'(v)}{f(v)}\frac{\partial}{\partial\theta}\right)$$

$$
\begin{aligned}
& + f'(v)\frac{\partial}{\partial\theta} \\
= & -\sin^2\theta\frac{\partial}{\partial u} + \sin\theta\cos\theta f(v)\frac{\partial}{\partial v} - \sin^2\theta f'(v)\frac{\partial}{\partial\theta} \\
& + f'(v)\frac{\partial}{\partial\theta} \\
= & -\sin^2\theta\frac{\partial}{\partial u} + \sin\theta\cos\theta f(v)\frac{\partial}{\partial v} + \cos^2\theta f'(v)\frac{\partial}{\partial\theta}. \qquad (2.12)
\end{aligned}
$$

This equation is valid before and after the turning point. We could establish a similar equation for Q before the turning point, but it is less clean and we will not use it.

2.4 Relation of Values to the Entry Angle

We demonstrate how some properties, from the size of the images of the differential to the time spent in the cap, relate to the angle of entry, α. These are the final *internal* tools of this chapter. The reader should also recall that $k \geq 3$ is the degree of the first non-zero derivative of f, the rotated function.

We start with the following definition that we use to simplify notation.

Definition 2.4.1. *We say that $f(\alpha) \asymp g(\alpha)$ if there exists a constant $C \geq 1$, independent of α, such that*

$$\frac{g(\alpha)}{C} \leq f(\alpha) \leq Cg(\alpha).$$

The next lemma tells us how the v-value at the turning point, $v_{\max}(\alpha)$, relates to the entry angle α. It follows from Clairaut's relation on page 15.

Lemma 2.4.1. *Let $v_{max}(\alpha)$ be the maximum v-value that a geodesic, with entry angle α, attains in the cap. Then, we have the following estimate*

$$v_{max}(\alpha) \asymp \alpha^{\frac{2}{k}}.$$

Proof: For α sufficiently small, there are constants C_1 and C_2 greater than 0, such that

$$f(0) - \frac{\alpha^2}{C_1} \leq f(0)\cos\alpha \leq f(0) - C_1\alpha^2$$

and

$$f(0) - \frac{v_{\max}^k(\alpha)}{C_2} \leq f(v_{\max}(\alpha)) \leq f(0) - C_2 v_{\max}^k(\alpha).$$

As we know that $f(v_{\max}(\alpha)) = f(0)\cos\alpha$, the result follows immediately. $\Diamond$

A direct consequence of this is the value of the derivative of f at $v_{\max}(\alpha)$. We frequently use this interplay between finding the v-value at particular places and immediate consequences on f'. This is significant because we see from Equation 2.10 that f' relates directly to the Jacobi fields.

Corollary 2.4.1. *For α sufficiently small,*

$$-f'\left(v_{max}(\alpha)\right) \asymp \alpha^{\frac{2k-2}{k}}.$$

Proof: By standard calculus, there is a $C > 1$, such that for v sufficiently small, $\frac{v^{k-1}}{C} \leq -f'(v) \leq Cv^{k-1}$. The rest follows from the previous result. $\Diamond$

Let $T_{\frac{1}{2}}(\alpha)$ be the time that it takes for a geodesic with entry angle α to arrive at $v_{\max}(\alpha)$. Notice that $T_{\text{full}}(\alpha) = 2T_{\frac{1}{2}}(\alpha)$, where $T_{\text{full}}(\alpha)$ is the time to exit the positive curvature part of the cap. We use Gauss-Bonnet theorem on geodesic triangles to establish a relationship between these times, $T_{\text{full}}(\alpha)$ and $2T_{\frac{1}{2}}(\alpha)$, and the entry angle. (There is a proof in [BG] for $k = 3$ using a completely different technique that could be generalized.)

Lemma 2.4.2. *For α sufficiently small,*

$$T_{\frac{1}{2}}(\alpha) \asymp \alpha^{\frac{2-k}{k}},$$

and hence the estimate holds for $T_{full}(\alpha)$ as well.

Proof: Consider the cap as unrolled in a neighborhood of $v = 0$ with metric as induced. Also consider the following three geodesics on the (u, v)-strip: (i) the one unrolled from the closed geodesic at the entrance of the cap, (ii) the one that enters at angle α and $u = 0$ (the time is the same for any u, so we can make this assumption), and (iii) the one that runs from $v = 0$ to $v = v_{\max}(\alpha)$ with u constant and meets the second geodesic when it reaches its peak. Let Δu be the u-value for geodesic (ii) at its peak. Since the angle with respect to the change in u coordinate is always small, Δu is approximately $T_{\frac{1}{2}}(\alpha)$ divided by $f(0)$. Thus, we actually

estimate Δu. The third geodesic meets the first two orthogonally. The first two geodesics meet at an angle of α. Hence, by the Gauss-Bonnet theorem on geodesic triangles, we have

$$\alpha = \iint_{\tau} \kappa d\sigma.$$

From our parameters, knowing that $\kappa(u,v) = \dfrac{-f''(v)}{f(v)}$ and the Jacobian is $f(v)$, we have

$$\alpha = \int_0^{\Delta u} \int_0^{v(u)} -f''(v) dv du.$$

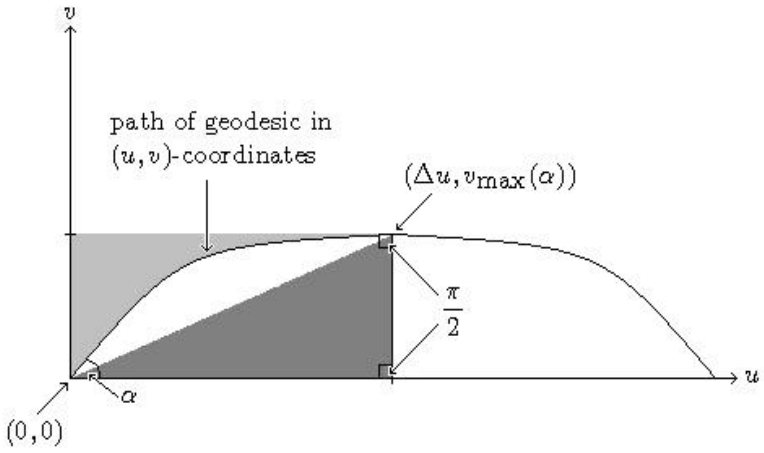

Figure 2.4.1. Over and underestimation of the integral of the curvature.

We over and underestimate this integral to obtain lower and upper bounds on Δu of the same order of magnitude, see Figure 2.4.1. For the overestimation, we use the box $[0, \Delta u] \times [0, v_{\max}(\alpha)]$. Then,

$$\begin{aligned} \alpha &\leq \int_0^{\Delta u} \int_0^{v_{\max}(\alpha)} -f''(v) dv du \\ &= \Delta u \left(-f'\left(v_{\max}(\alpha)\right)\right). \end{aligned}$$

This implies that

$$\begin{aligned}\Delta u &\geq \frac{\alpha}{\left(-f'\left(v_{\max}(\alpha)\right)\right)} \\ &\geq \frac{\alpha^{\frac{2-k}{k}}}{C},\end{aligned}$$

where C comes from Corollary 2.4.1.

For the underestimation, note that the slope of $v(u)$ is

$$\frac{\frac{dv}{dt}}{\frac{du}{dt}} = \tan\theta f(v) = \tan\theta \sec\theta f(0)\cos\alpha.$$

Since θ is decreasing, the curve $v(u)$ is concave down. Therefore, it lies above the linear equation in the (u, v)-coordinates containing the values $(0, 0)$ and $(\Delta u, v_{\max}(\alpha))$. So,

$$\begin{aligned}\alpha &\geq \int_0^{\Delta u}\int_0^{\frac{v_{\max}(\alpha)}{\Delta u}u} -f''(v)dvdu \\ &= \int_0^{\Delta u} -f'\left(\frac{v_{\max}(\alpha)}{\Delta u}u\right)du \\ &= \Delta u\frac{\left(f(0) - f\left(v_{\max}(\alpha)\right)\right)}{v_{\max}(\alpha)} \\ &= \Delta u\frac{\left(f(0) - f\left(0\right)\cos\alpha\right)}{v_{\max}(\alpha)}.\end{aligned}$$

As above, we can manipulate and get

$$\begin{aligned}\Delta u &\leq \frac{\alpha v_{\max}(\alpha)}{\left(f(0) - f\left(0\right)\cos\alpha\right)} \\ &\leq \tilde{C}\alpha^{\frac{2-k}{k}},\end{aligned}$$

where $\tilde{C}$ comes from the appropriate estimates from lemma 2.4.1 and of $1 - \cos\alpha$. The rest comes from the fact that $\dfrac{du}{dt} = \dfrac{\cos\theta}{f(v)}$ is between positive constants for α small. $\Diamond$

We now look backwards in the region of the caps with negative curvature, that is to say where $v < 0$. We use Equations 2.10 and 2.11 to estimate the form of the cones as they are pushed forward to the frontier of the positive curvature. This gives estimates on the linear combination of Q and H that form the unstable

vectors, which helps control growth through the positive curvature region.

Lemma 2.4.3. *Let x have footprint in the closed geodesic at $v = 0$ and $V \neq 0 \in T_xSM$. Furthermore, let $R(x)$ denote the ratio of the of vertical to horizontal components of V. If $D\phi_t V$ remains in $C(\phi_t(x))$ for $t \leq 0$, then*

$$R(x) \asymp \alpha^{\frac{k-2}{k}}.$$

Proof: To estimate $R(x)$ from above, we find the composition of $H(v)$ and $Q(v)$ so that

$$\tilde{J}_1(v_2(\alpha)) = a_1 H(v_2(\alpha)) + b_1 Q(v_2(\alpha)) = (0, 1).$$

Here, $v_2(\alpha)$ is the v at which we have $\theta = 2\alpha$. By direct computation, the coefficients are $a_1 = -q(v_2(\alpha))$ and $b_1 = h(v_2(\alpha))$. Therefore, the ratio of the vertical to horizontal part for vectors, which rest in the cones for negative time, is less than that of

$$\tilde{J}_1(0) = \left(-q(v_2(\alpha)) f(0) \sin\alpha, \frac{h(v_2(\alpha))}{f(0)\sin\alpha} \right).$$

To estimate the ratio, we first estimate $v_2(\alpha)$. Similar to Lemma 2.4.1, for α small, we have the following estimates:

$$\frac{\alpha^2}{C_1} \leq f(0)(\cos\alpha - \cos 2\alpha) \leq C_1\alpha^2,$$

and for $v < 0$

$$f(0) + \frac{(-v_2(\alpha))^k}{C_2} \leq f(v_2(\alpha)) \leq f(0) + C_2(-v_2(\alpha))^k.$$

Manipulating $f(v_2(\alpha))\cos 2\alpha = f(0)\cos\alpha$ and subtracting $f(0)\cos 2\alpha$ from both sides gives us

$$-v_2(\alpha) \asymp \alpha^{\frac{2}{k}}.$$

To overestimate $R(x)$, we will underestimate the ratio of horizontal to vertical.

For some constant C, we have the following:

$$\begin{aligned}
\frac{\tilde{J}_{1H}(0)}{\tilde{J}_{1V}(0)} &= \frac{-q(v_2(\alpha))f^2(0)\sin^2\alpha}{h(v_2(\alpha))} \\
&= \int_{v_2(\alpha)}^{0} \frac{1}{f^2(s)\sin^3\theta} ds f^2(0)\sin^2\alpha \\
&\geq \int_{v_2(\alpha)}^{0} \frac{1}{2f^2(0)\sin^3 2\alpha} ds f^2(0)\sin^2\alpha \\
&= -v_2(\alpha)\frac{2\sin^2\alpha}{\sin^3 2\alpha} \\
&\geq C\alpha^{\frac{2-k}{k}}.
\end{aligned}$$

Thus, the ratio of the vertical to horizontal satisfies

$$R(x) \leq \tilde{C}\alpha^{\frac{k-2}{k}}.$$

For the other side of the inequality, consider

$$\tilde{J}_2(v_2(\alpha)) = a_2 H(v_2(\alpha)) + b_2 Q(v_2(\alpha)) = (1,0)\,.$$

Again by direct computation, the coefficients are $a_2 = \dfrac{1}{h(v_2(\alpha))}\left(1 + f'(v_2(\alpha))q(v_2(\alpha))\right)$ and $b_2 = -f'(v_2(\alpha))$. Now this gives us

$$\tilde{J}_2(0) = \left(\frac{(1 + f'(v_2(\alpha))q(v_2(\alpha)))}{h(v_2(\alpha))} f(0)\sin\alpha, \frac{-f'(v_2(\alpha))}{f(0)\sin\alpha}\right).$$

Similar to above, we overestimate the ratio of horizontal to vertical. Using that $-f'(v_2(\alpha)) \asymp \alpha^{\frac{2k-2}{k}}$, we have

$$\begin{aligned}
\frac{\tilde{J}_{2H}(0)}{\tilde{J}_{2V}(0)} &= \frac{\left(1 + f'(v_2(\alpha))q(v_2(\alpha))\right) f^2(0)\sin^2\alpha}{-f'(v_2(\alpha))h(v_2(\alpha))} \\
&\leq \frac{f^2(0)\sin^2\alpha}{-f'(v_2(\alpha))h(v_2(\alpha))} \\
&\leq C'\alpha^{\frac{2-k}{k}}.
\end{aligned}$$

By inversion, we get

$$R(x) \geq \tilde{C}'\alpha^{\frac{k-2}{k}}.$$

This, together with the overestimation, gives the result. $\Diamond$

The next result yields control on the size of the vector Q before the turn. This is useful in controlling the size of vectors that remain in the complement cones. In order to derive this result, we use the explicit form of Q and the discussion on page 12 that allows us to locate maximums.

Lemma 2.4.4. *For α sufficiently small, there exists a constant C such that*

$$\|Q(v)\| \leq C\alpha^{\frac{2-2k}{k}}$$

for $v \leq v_{max}(\alpha)$.

Proof: The maximum in the first "half" occurs where the vertical part is 0. By Equation 2.11, we know that the maximum of $\|Q(v)\|$ occurs at a v_s where

$$q(v_s) = -\frac{1}{f'(v_s)}.$$

There are two possibilities for v_s:

1. $v_s \leq v_{\frac{1}{2}}$, or
2. $v_{\frac{1}{2}} < v_s \leq v_{max}$,

where $v_{\frac{1}{2}} = v_{\frac{1}{2}}(\alpha)$ is the v at which we have $\theta = \dfrac{\alpha}{2}$.

Just as in Lemma 2.4.3, we first estimate $v_{\frac{1}{2}}$ by using

$$\frac{\alpha^2}{C_1} \leq f(0)\left(\cos\frac{\alpha}{2} - \cos\alpha\right) \leq C_1\alpha^2,$$

and for $v > 0$

$$f(0) - \frac{\left(v_{\frac{1}{2}}\right)^k}{C_2} \leq f\left(v_{\frac{1}{2}}\right) \leq f(0) - C_2\left(v_{\frac{1}{2}}\right)^k.$$

Manipulating $-f\left(v_{\frac{1}{2}}\right)\cos\frac{\alpha}{2} = -f(0)\cos\alpha$ and adding $f(0)\cos\dfrac{\alpha}{2}$ to both sides yields

$$v_{\frac{1}{2}} \asymp \alpha^{\frac{2}{k}}.$$

If $v_s \leq v_{\frac{1}{2}}$, we can estimate $q(v_s)$ directly:

$$\begin{aligned} q(v_s) &= f(v_s)\sin\theta \int_0^{v_s} \frac{1}{f^2(s)\sin^3\theta} ds \\ &\leq f(0)\sin\alpha \int_0^{v_s} \frac{1}{f^2(v_s)\sin^3\frac{\alpha}{2}} ds \\ &\leq C\alpha^{-2} \int_0^{v_{\frac{1}{2}}} 1 ds \\ &= C\alpha^{-2} v_{\frac{1}{2}} \\ &\leq \tilde{C}\alpha^{\frac{2-2k}{k}} \end{aligned}$$

If $v_{\frac{1}{2}} < v_s \leq v_{max}$, we can estimate

$$-\frac{1}{f'(v_s)} \leq -\frac{1}{f'\left(v_{\frac{1}{2}}\right)}$$

instead of $q(v)$. Similar to Corollary 2.4.1, we have $-f'\left(v_{\frac{1}{2}}\right) \asymp \alpha^{\frac{2k-2}{k}}$. This in turn implies

$$q(v_s) = -\frac{1}{f'(v_s)} \leq C\alpha^{\frac{2-2k}{k}}.$$

Combining the two estimates,

$$\max_{0\leq v\leq v_{max}} \{\|Q(v)\|\} = q(v_s) \leq C\alpha^{\frac{2-2k}{k}}$$

as desired. $\Diamond$

We put several of these results together in order to get good estimates on the size of H and Q at the turning point. Notice that Q has grown proportionally to the decay of H. These estimates are used to calculate angles between vectors of interest. This control on angles enables us to understand how the unstable manifolds go through the region with footprint in the positive curvature part of the cap.

Corollary 2.4.2. *The norm of H and Q at $v_{max}(\alpha)$ satisfies*

$$\|H(v_{max}(\alpha))\| \asymp \alpha^{\frac{2k-2}{k}}$$

and

$$\|Q\left(v_{max}(\alpha)\right)\| \asymp \alpha^{\frac{2-2k}{k}},$$

respectively.

Proof: Follows from Lemma 2.4.4, Corollary 2.4.1, and the form of Q and H. $\Diamond$

2.5 Essential Properties of the Flow

Here, we develop most of the properties that are used by the subsequent chapters. Many of them deal with the long term behavior of the differential on vectors in the cones. The consequences of the main results can be summarized in the following two phrases: (i) The unstable vectors grow in the long run, and we can estimate how much they might shrink. (ii) The stable vectors do not grow significantly and decay in the long run.

The first proposition gives us the non-growth of the stables. It is stated first in terms of the vectors that remain in the cones in negative times. It follows from our estimates on the size of the vectors presented in Section 2.4 and from Lemma 2.2.2, giving us a dichotomy on where the maximum can occur. We show that *effectively* the maximum of the norm of the vector must occur as the orbit leaves the region of positive curvature.

Proposition 2.5.1. *There exists a constant $K_1 > 0$ such that if the following hold:*

1. *$x \in U$ and $V \in C(x)$ and*
2. *$D\phi_t(x)V \in C\left(\phi_t(x)\right)$ for all times $t \leq 0$ with $\phi_t(x) \in U$,*

then

$$\|D\phi_t(x)V\| \leq K_1\|V\|$$

for all $t \leq 0$.

Proof: Anytime $\phi_t(x) \in U$, we have the estimate for $K = 1$. So, the important estimate is for the time spent in the caps. Considering the flow moving in negative time, let $\tilde{V}$ be the image of V at the time that the orbit is about to exit the cap.

By Corollary 2.2.1, $\|V\| \geq \|\tilde{V}\|$. Since V remains in the cones for negative time (and hence $\tilde{V}$), Lemma 2.4.3 implies that the ratio of the vertical to horizontal part of $\tilde{V}$ is less than $\tilde{C}\alpha^{\frac{k-2}{k}}$. Normalize so that $\tilde{V}$ can be written

$$\tilde{V} = \frac{H(0)}{f(0)\sin\alpha} + \epsilon f(0)\sin\alpha Q(0)$$

with $\epsilon \leq \tilde{C}\alpha^{\frac{k-2}{k}}$. By Lemma 2.4.4, we have for $0 \leq v \leq v_{max}$,

$$\begin{aligned}
\left\| \frac{H(v)}{f(0)\sin\alpha} + \epsilon f(0)\sin\alpha Q(v) \right\| &\leq \frac{\|H(v)\|}{f(0)\sin\alpha} + \epsilon f(0)\sin\alpha \max_{0\leq v\leq v_{max}} \{||Q(v)||\} \\
&\leq 1 + \epsilon f(0)\sin\alpha C \frac{1}{\alpha^{\frac{2k-2}{k}}} \\
&\leq 1 + C\tilde{C}\alpha^{\frac{k-2}{k}} \frac{1}{\alpha^{\frac{k-2}{k}}} \\
&= 1 + C\tilde{C} \\
&\leq \left(1 + C\tilde{C}\right)\|\tilde{V}\| \\
&\leq \left(1 + C\tilde{C}\right)\|V\|.
\end{aligned}$$

Using Lemma 2.2.2, the maximum is either achieved before the turn or $\|V\|$ is the maximum. $\Diamond$

Immediately, we restate this in terms of vectors in the complement cones.

Corollary 2.5.1. *There exists a constant K_2 such that if the following hold:*

1. *$x \in U$ and $V \in \widehat{C}(x)$, and*
2. *$D\phi_t V \in \widehat{C}\left(\phi_t(x)\right)$ for all times $t \geq 0$ with $\phi_t(x) \in U$,*

then

$$\|D\phi_t V\| \leq K_2\|V\|,$$

for all $t \geq 0$.

Proof: This follows from symmetry. $\Diamond$

The next corollary gives us control of the decay of unstable vectors. It depends on how far, from the region of positive curvature, the orbit starts. We combine Corollary 2.5.1 with the fact that the flow preserves the standard symplectic form.

For $\delta > 0$, let U_δ be defined by

$$U_\delta = \{x \in U | d(x, \partial U) \geq \delta\}.$$

Corollary 2.5.2. *For $\delta > 0$, there is a $C(\delta) > 0$ such that if $x \in U_\delta$ and $V \in C(x)$ then for $t \geq 0$*

$$\|D\phi_t V\| \geq C(\delta)\|V\|.$$

Proof: We simply need to show that if the orbit passes through the cap, the condition holds. For $x \in U_\delta$, there is a minimum angle formed between any $V \in C(x)$ and the image of the complement cones having already passed through the cap. Let $\beta_{min}(\delta)$ be this minimum angle. Furthermore, let

$$W \in \bigcap_{t \geq 0} D\phi_{-t}\widehat{C}(\phi_t(x))$$

be normalized and $\beta(t)$ be the angle between $D\phi_t V$ and $D\phi_t W$. Then by preservation of area and Corollary 2.5.1, we have

$$\begin{aligned} \|D\phi_t V\| \|D\phi_t W\| \sin\beta(t) &= \|V\| \sin\beta(0) \\ &\geq \|V\| \sin\beta_{min}(\delta) \end{aligned}$$

and hence

$$\begin{aligned} \|D\phi_t V\| &\geq \|V\| \frac{\sin\beta_{min}(\delta)}{\|D\phi_t W\| \sin\beta(t)} \\ &\geq C(\delta)\|V\|. \ \Diamond \end{aligned}$$

In the following proposition, we give a qualitative description of the behavior of the flow in a neighborhood of the *singular set* N. The singular set is the collection of orbits, $\mathcal{O}(y)$, that project down to the closed geodesics separating the regions of positive and negative curvature. The closed orbits come in pairs, two per cap, by following the geodesic in both directions. This is a consequence of the structure given to us by the level sets of the Clairaut equation. Let $\mathcal{O}(y)_\epsilon$ denote an ϵ neighborhood of $\mathcal{O}(y)$.

Proposition 2.5.2. *There exist weak-stable and weak-unstable manifolds of $y \in N$ contained in U. For ϵ small, they split $\mathcal{O}(y)_\epsilon \bigcap cl(U)$ into three regions. The first region, denoted U_{in}, is bordered by the weak-stable and the boundary of U. The*

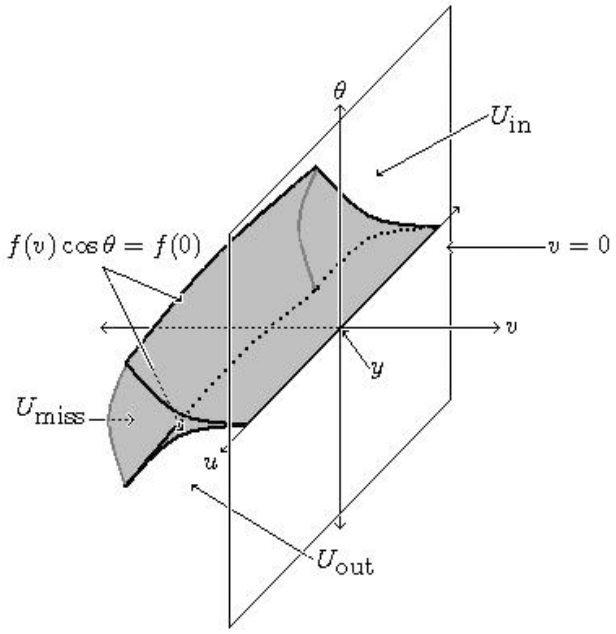

Figure 2.5.1. Splitting of U near orbits in N.

second region, denoted U_{miss}, is bordered by the weak-stable and weak-unstable. The third region, denoted U_{out}, is bordered by the weak-unstable and the boundary of U (see Figure 2.5.1).

The orbits of $x \in U_{in}$ approach $\mathcal{O}(y)$ and ∂U until they enter the complement of U. In the complement of U, the orbit remains in the neighborhood $\mathcal{O}(y)_{g(\epsilon)}$, for some function g that decays with ϵ, until it enters U_{out}. The same happens for $x \in U_{out}$ in negative time. The x in U_{miss} leave the neighborhood $\mathcal{O}(y)_\epsilon$ without leaving U in both negative and positive times.

Proof: In a neighborhood $\mathcal{O}(y)_\epsilon$, the Clairaut surface, $\{(u, v, \theta) \,|\, \cos\theta f(v) = f(0)\}$, give the weak-stable and weak-unstable manifolds of y. The weak-stable manifold is the subset where $\sin\theta \geq 0$ and the weak-unstable manifold is the subset where $\sin\theta \leq 0$. In $\mathcal{O}(y)_\epsilon \bigcap cl\,(U)$, U_{in} and U_{out} are given by the conditions $\cos\theta f(v) < f(0)$ with $\sin\theta > 0$ and $\sin\theta < 0$ respectively. U_{miss} is given by the condition $\cos\theta f(v) > f(0)$. They all clearly have the desired properties. $\Diamond$

The next property will be frequently referred to as the *dichotomy property.* It largely follows from the above property. It basically assures that the behavior in U dominates all of the orbits except those in the singular set.

Proposition 2.5.3. *There exists a $\widehat{\epsilon} > 0$, with the dichotomy that for $x \in S\tilde{M}$, either x always returns to $U_{\widehat{\epsilon}}$ (as on page 28) or x lies on the weak-stable for some y in N.*

Proof: The $\widehat{\epsilon}$ comes from the size of the negative curvature part of the surfaces of revolution and the rest follows from the proof of Proposition 2.5.2. $\Diamond$

Putting this dichotomy property to use for the first time, we get a core result that the unstable vectors live up to their name and grow.

Corollary 2.5.3. *For $x \in U$ and $V \in C(x)$,*

$$\lim_{t\to\infty} \|D\phi_t V\| = \infty.$$

Proof: There are two possibilities, the first is that x eventually lies on a local stable of some $y \in N$. Then the property is obvious, the V would grow at least linearly in the long term behavior; after some time it would remain in negative curvature. Otherwise, we get the result by Proposition 2.5.3, Corollary 2.5.2, and that the returns to the complement of $U_{\widehat{\epsilon}}$ are bounded below. $\Diamond$

Similarly, we can determine that the stable vectors decay. Note this is neither stronger than, nor implied directly by Corollary 2.5.2. The key is the dichotomy property.

Corollary 2.5.4. *For $x \in U$ and V such that $D\phi_t V \in \widehat{C}\,(\phi_t(x))$, for all $t \geq 0$, then*

$$\lim_{t\to\infty} \|D\phi_t V\| = 0.$$

Proof: There are two possibilities, the first is that x eventually lies on a local stable of some $y \in N$. Then the property is obvious geometrically. Otherwise, by Proposition 2.5.3, that returns to the complement of $U_{\widehat{\epsilon}}$ is bounded below, and Corollary 2.5.1, we have the property via the fact that there is uniform growth in the cones in $U_{\widehat{\epsilon}}$. $\Diamond$

We can extend the cones naturally to the $z \in N$ by the same property that defines the cones in U. Since the footprint of the orbit of z remains in zero curvature, the cones remain invariant and converge by intersection to the horizontal distribution. Let $D^u(z)$ be this distribution. In Chapter 3, we see that the unstable

distribution cannot be extended continuously in a neighborhood of N. However, the following lemma is used to show that from the U-side it has a continuous extension.

Proposition 2.5.4. *For $x \in cl(U) \setminus N$ there exists a time $t = t(x)$ such that $D\phi_t\left(C\left(\phi_{-t}(x)\right)\right)$ converge to $D^u(z)$ as x converges to $z \in N$.*

Proof: We only need to consider x in a neighborhood of N. For $x \in U_{\text{miss}}$ and $x \in U_{\text{in}}$ it is clear, we can choose $t(x)$ as the time it took the orbit of x to move from U_ϵ to the position x. For the $x \in U_{\text{out}}$, we can consider the time it took it to move from U_ϵ, through U_{in} and the complement of U, to its current position. By Corollary 2.2.1 and symmetry, the cone is closer to horizontal than the one at the symmetric position in U_{in}. $\Diamond$

The following proposition does not follow from the previous work. It is a couple of basic properties of the system that we use in the chapters to come. They follow from the main result of [BG]. We include them here to keep the core properties of the system consolidated. We define $x \in M$ to be an *attractive orbit* if there is an open set O and $\delta < \infty$ such that $\phi_t(O)$ approaches $\phi_t\left(\bigcup_{|s|\leq\delta} \phi_s(x)\right)$ as $t \to \infty$.

Proposition 2.5.5. *The flow ϕ_t is topologically transitive and has no attractive orbits.*

Proof: In [BG], it is shown that the flow is Bernoulli with respect to volume, which is stronger than these conditions. $\Diamond$

2.6 Proof of Lemma 3.4.4 in Local Coordinates

We complete this chapter with a proof of a restatement of Lemma 3.4.4. We use some results from Chapter 3, which are shown in more generality than most of the proofs here. This lemma is more natural to prove in local coordinates and is consistent with the overall philosophy of this work: to interplay basic general properties with local analysis for technical problems. One should consult the results before Lemma 3.4.4 in Section 3.4.

The basic idea of the proof is to break the integral of the unstable into two parts: where the θ is positive and negative. Equivalently, one can say we break

it into the parts before and after their turning points. The first part is short by saying that the horizontal component (and hence the v component) is of fixed size. For the second part, if v is increasing in the integral, then the vertical must be of a certain size (and hence the change in θ).

Consider the local unstable given from the weak-stable of $y \in N$ into U_{in}, from U_{in} into the complement of U, and from the complement of U into U_{out}. This is possible by reversing orientation of Lemma 3.4.2 and by the proof of Lemma 3.4.3. Furthermore, by Proposition 2.5.2, we know that this curve remains in a neighborhood of $\mathcal{O}(y)$. Let $\alpha(s)$ represent the entry angle for the point s along this curve (notice this is given by the points Clairaut surface).

Lemma 2.6.1. *The value $\alpha(s)$ is always increasing.*

Proof: The unstable vector is transversal to the Clairaut surfaces. $\Diamond$

This next lemma is used to control the length in the region where $\theta > 0$. It uses basic information about the profile of differential image of vectors before the turning point and the respective sizes at the turning point.

Lemma 2.6.2. *In the region where $\theta \geq 0$, for α small, the horizontal component of the normalized unstable vector is greater than a positive constant.*

Proof: First note that the horizontal components increase and then decrease for the normalized vectors in the cones, as they move along before the turning point. Consequently, we only need the estimates at $v = 0$ and $v = v_{\max}(\alpha)$. At $v = 0$ it is obvious. To estimate the horizontal component at $v_{\max}(\alpha)$, let ϕ_0 be the angle between $H(0)$ and $V(0)$, and $\phi_{v_{\max}(\alpha)}$ be the angle between $H\left(v_{\max}(\alpha)\right)$ and $V\left(v_{\max}(\alpha)\right)$. Because the flow preserves the contact structure, we know that

$$\|H\left(v_{\max}(\alpha)\right)\|\|V\left(v_{\max}(\alpha)\right)\| \sin \phi_{v_{\max}(\alpha)} = \|H(0)\|\|V(0)\| \sin \phi_0.$$

By Lemma 2.4.3, Corollary 2.4.2, and the definition of H, we have

$$\frac{1}{C} \leq \frac{\|V(0)\|}{\|V\left(v_{\max}(\alpha)\right)\|} \leq C,$$

$$\frac{\alpha^{\frac{2-k}{k}}}{C} \leq \frac{\|H(0)\|}{\|H\left(v_{\max}(\alpha)\right)\|} \leq C\alpha^{\frac{2-k}{k}},$$

and

$$\frac{\alpha^{\frac{k-2}{k}}}{C} \leq \sin\phi_0 \leq C\alpha^{\frac{k-2}{k}}.$$

These imply that

$$\sin\phi_{v\max(\alpha)} = \frac{\|H\left(v_{\max}(\alpha)\right)\|\|V\left(v_{\max}(\alpha)\right)\|}{\|H(0)\|\|V(0)\|\sin\phi_0} \geq C',$$

with C' being a nonzero constant. The result follows since $H\left(v_{\max}(\alpha)\right)$ is the vertical down vector. $\Diamond$

The following result will be used to control the length in the region $\theta < 0$. It uses the same tools as Lemma 2.6.2, but spins off of Q instead of H.

Lemma 2.6.3. *The unstable vector has a ratio of vertical to horizontal of at least* $C\alpha^{\frac{k-2}{k}}$ *at* $v_{max}(\alpha)$.

Proof: Similar to the proof above, let ϕ_0 be the angle between $V(0)$ and $Q(0)$ and let $\phi_{v\max(\alpha)}$ be the angle between and $V\left(v_{\max}(\alpha)\right)$ and $Q\left(v_{\max}(\alpha)\right)$. We have

$$\begin{aligned}\sin\phi_{v\max(\alpha)} &= \frac{\|Q(0)\|\|V(0)\|\sin\phi_0}{\|Q\left(v_{\max}(\alpha)\right)\|\|V\left(v_{\max}(\alpha)\right)\|} \\ &\geq C\alpha^{\frac{k-2}{k}}.\end{aligned}$$

Since $Q\left(v_{\max}(\alpha)\right)$ is below the horizontal, we get the result. $\Diamond$

We finally have the tools to prove the main result of this section. This result gives us the desired behavior in a neighborhood of the singular sets.

Proposition 2.6.1. *The length of the unstable curve going outside of* U *goes to zero as* x *approaches the singular set* N.

Proof: As we have a focusing cap, all the unstable vectors, at the $\theta = 0$ cross section, have vertical component negative. Thus, an unstable curve can intersects this cross section precisely once (see the proof of Lemma 3.4.3). All elements of the cross section are at their turning point. Let α_0 be the entering angle of the point where the curve intersects this section.

By Lemma 2.6.2, the horizontal component of the unstable vector is at least $0 < C < 1$ in the region where $\theta \geq 0$. Equation 2.5 implies that the v-component is at least $C\cos\alpha_0$. Since the v-value varies from 0 to $v_{\max}(\alpha_0)$, the total length

of the curve in this region is less than $\frac{v_{\max}(\alpha_0)}{C\cos\alpha_0}$. Lemma 2.4.1 implies that this fraction goes to zero at a rate of $\alpha^{\frac{2}{k}}$.

Now we turn to the part of the curve where $\theta < 0$. Notice that the parameter of α as it exits, α_{exit}, satisfies $\alpha_0 < \alpha_{\text{exit}} < C_2\alpha_0$. This follows from the time estimates of Lemma 2.4.2, Lemma 2.6.1. Due to positive curvature, a normalized vector has vertical component decreasing until it reaches -1. Hence using Lemma 2.6.3 and the fact that $\alpha(s)$ is increasing, the vertical component is less than $-C\alpha_0^{\frac{k-2}{k}}$ when the vector has positive horizontal component.

Divide the curve into components where v is increasing, and where v is non-increasing. For the parts where v is increasing, the horizontal component is positive. By Equation 2.5, the shift in the θ direction is at least $-C\alpha_0^{\frac{k-2}{k}}l$, where l is the length of the curve with v-component positive. Since the θ shift is bounded by α_{exit}, we have $l \leq C_1\alpha_0^{\frac{2}{k}}$.

For the parts where v is non-increasing, by Equation 2.12 and the fact that the vector cannot "pass" H, θ and v components are monotonic and the total shift for each is bounded by $C_2\alpha_0$ and $C_3\alpha_0^{\frac{2}{k}}$ respectively. These bound the length of the components where v is non-increasing by a constant times $\alpha_0^{\frac{2}{k}}$. This finishes the proof. $\Diamond$

Chapter 3

Existence and Properties of Unstable and Weak-Unstable Manifolds

The main objects, on which later constructions occur, are built in this chapter. The notation is formalized and we establish basic structural properties, which are used when we examine the dynamic properties in Chapter 4. Corollary 3.5.3 is the core estimate of this chapter as it is the germ of holonomy invariance of the weak-unstable conditional measure.

Most properties are shown for the unstable manifolds. However, due the symmetry of the conditions (in fact for geodesic flows, the flow is symmetric), all of the properties hold for the stable manifolds as well. They are used for the latter without further mention.

3.1 Basic Setup, Notations, and Properties

We concisely restate some of the objects and properties proven in Chapter 2 in a notation consistent for the remaining chapters. This collection of properties is a starting point for examining other systems that have some of the same behaviors. Many systems have some of the core properties and thus the overall construction should be adaptable. We do not give notations for any objects that are not yet constructed, so this should not be considered as a complete collection of notation.

We consider M to be a three dimensional Riemannian manifold with a C^2 metric. Let ϕ_t be a unit speed C^2 flow, and $D\phi_t$ denote its differential. Let TM be

the tangent bundle and $T^{\perp}M$ be the sub-bundle orthogonal to the flow direction. The properties of the geodesic flows, shown in Chapter 2, are the following.

Property 3.1.1. *There exists an open set U and a set of continuously varying cones $C(x) \subset T_x^{\perp}M$ for $x \in U$ with the following characteristics:*

1. *$D\phi_t C(x) \subset C\left(\phi_t(x)\right)$ whenever $\phi_t(x) \in U$,*
2. *if $x \in U$ then the orbit of x always returns to U, and*
3. *the complement $N = M \setminus \bigcup_{t \geq 0} \phi_t(U)$ is a finite collection of isolated closed orbits.*

Let $\widehat{C}(x)$ denote the complement cone of $C(x)$ in $\subset T_x^{\perp}M$. As before, N is referred to as the *singular set*; terminology of this becomes more clear in the next section. Let

$$M_0 := M \setminus N$$

be the open sub-manifold of M outside of the singular set.

For $\epsilon > 0$ and $A \subset M$, we use

$$B_\epsilon(A)$$

to denote the ball of radius ϵ about A and let

$$M_\epsilon := M \setminus B_\epsilon(N)$$

be the set at least ϵ away from the singular set. Notice that M_ϵ is a compact subset. For periodic points $x \in M$, $\mathcal{O}(x)$ denotes the orbit of x. Finally, because it is used heavily to simplify equations in later chapters, we define

$$\beta(s) := \max_{|t| \leq s} \left\{ ||D\phi_t|| \right\},$$

which is an upper bound on growth of tangent vectors for times less than s.

Property 3.1.2. *There exists a constant $K > 0$ such that if the following hold:*

1. *$x \in U$ and $V \in C(x)$, and*

2. $D\phi_t(x)V \in C\left(\phi_t(x)\right)$ *for all times* $t \leq 0$ *with* $\phi_t(x) \in U$*,*

then

$$\|D\phi_t(x)V\| \leq K\|V\|$$

for all $t \leq 0$*.*

Property 3.1.3. *For* $\delta > 0$*, there is a* $C(\delta) > 0$ *such that if* $x \in U_\delta$ *and* $V \in C(x)$ *then for* $t \geq 0$

$$\|D\phi_t V\| \geq C(\delta)\|V\|.$$

Property 3.1.4. *There exist weak-stable and weak-unstable manifolds of* $y \in N$ *contained in* U*. For* ϵ *small, they split* $\mathcal{O}(y)_\epsilon \bigcap cl\left(U\right)$ *into three regions. The first region, denoted* U_{in}*, is bordered by the weak-stable and the boundary of* U*. The second region, denoted* U_{miss}*, is bordered by the weak-stable and weak-unstable. The third region, denoted* U_{out}*, is bordered by the weak-unstable and the boundary of* U *(see Figure 2.5.1).*

The orbits of $x \in U_{in}$ *approach* $\mathcal{O}(y)$ *and* ∂U *until they enter the complement of* U*. In the complement of* U*, the orbit remains in the neighborhood* $\mathcal{O}(y)_{g(\epsilon)}$*, for some function* g *that decays with* ϵ*, until it enters* U_{out}*. The same happens for* $x \in U_{out}$ *in negative time. The* x *in* U_{miss} *leave the neighborhood* $\mathcal{O}(y)_\epsilon$ *without leaving* U *in both negative and positive times.*

Property 3.1.5. *There exists a* $\widehat{\epsilon} > 0$*, with the dichotomy that for* $x \in S\tilde{M}$*, either* x *always returns to* $U_{\widehat{\epsilon}}$ *or* x *lies on the weak-stable for some* y *in* N*.*

Property 3.1.6. *For* $x \in U$ *and* $V \in C(x)$*,*

$$\lim_{t\to\infty} \|D\phi_t V\| = \infty.$$

Property 3.1.7. *For* $x \in U$ *and* V *such that* $D\phi_t V \in \widehat{C}\left(\phi_t(x)\right)$*, then*

$$\lim_{t\to\infty} \|D\phi_t V\| = 0.$$

For us, a *distribution* is a one dimensional subspace in the tangent plane.

Property 3.1.8. *There exist distributions $D^u(z) \subset T_z^{\perp}M$ tangent to the weak stable of $z \in N$. Furthermore, for all $x \in cl(U) \setminus N$ there exists a time $t = t(x)$ such that $D\phi_t\left(C\left(\phi_{-t}(x)\right)\right)$ converge to $D^u(z)$ as x converges to $z \in N$.*

We define $x \in M$ to be an *attractive orbit* if there is an open set O and $\delta < \infty$ such that $\phi_t(O)$ approaches $\phi_t\left(\bigcup_{|s|\leq\delta} \phi_s(x)\right)$ as $t \to \infty$.

Property 3.1.9. *The flow ϕ_t is topologically transitive and has no attractive orbits.*

Property 3.1.10. *All of the previous properties hold if we take ϕ_{-t} and reverse the roles of $C(x)$ and $\widehat{C}(x)$.*

Property 3.1.11. *Local analysis around the singular set is used to get Lemma 3.4.4.*

3.2 Existence and Uniqueness of Local and Global Unstable Manifolds

In this section, we establish the existence and continuity of local unstable manifolds. They are realized as an integral of a continuous vector field. The key is uniqueness from Proposition 3.2.2. In the process, we establish that the size of stable vectors can be made uniformly small under the flow on compact sets, despite the fact that the system is non-uniformly hyperbolic. This is a powerful tool that we use frequently. We close with a construction of the global unstable manifolds and local weak-unstable manifolds. In [VD2][1], there is a different construction of stable and unstable manifolds that relies on certain estimates on the time of returns to U and results in knowledge of their existence only at certain points.

In order to construct the unstable manifolds, we first show that we have a natural distribution that gives an unstable direction. Since a distribution is one dimensional, we are able to build locally the unstable manifolds by realizing the distribution as a continuous unit length vector field.

[1] V. Donnay uses a Hadamard-Perron argument.

The metric we use on the cones is given by

$$d\left(C_1, C_2\right) = d_H\left(\tilde{C}_1, \tilde{C}_2\right),$$

where $\tilde{C}_j$ is the intersection of C_j with SM, $j = 1, 2$ and d_H is the Hausdorff distance. So for x in U, lets consider the intersection of the images of cones

$$D^u(x) = \bigcap_{\{t \geq 0 | \phi_{-t}(x) \in U\}} D\phi_t C\left(\phi_{-t}(x)\right).$$

Proposition 3.2.1. *The above gives a continuous invariant distribution in U.*

Proof: The set $D^u(x)$ is nonempty because the sets are nested and contain a nested sequence of compact subsets in the unit tangent space. It is invariant on returns to U by construction and any vectors in it rest in the unstable cones for all negative time. Property 3.1.2 implies that any vectors in D^u would have bounded growth in negative time. Thus, it cannot contain linearly independent vectors because they would span the orthogonal tangent space and hence all vectors would have bounded growth in negative time, contradicting a variant of Property 3.1.6.

Finally for continuity, consider $x \in U$. For any $\epsilon > 0$, we can find a t such that the cone $D\phi_t C\left(\phi_{-t}(x)\right)$ is $\dfrac{\epsilon}{2}$ close to the distribution. By continuity, we have that, in some small neighborhood, the $D\phi_t$ images of cones from some neighborhood of the preimage of x are $\dfrac{\epsilon}{2}$ close to $D\phi_t C\left(\phi_{-t}(x)\right)$. Hence any distribution contained in these cones would be ϵ close to $D^u(x)$. $\diamondsuit$

Now one can extend D^u to all of M_0 by defining the distribution at a point y to be the image of the distribution under $D\phi_t$ for any $x \in U$ with $\phi_t(x) = y$. By invariance, this is unique and continuity follows immediately from the continuity in U.

The next lemma shows that we can make stable vectors uniformly small on a compact subset of M_0. This should not be interpreted to mean that the decay can be made uniform everywhere, which is not true.

Lemma 3.2.1. *Let A be any compact subset of M_0 and $S(x)$ be the selection of one of the two unit length vectors in $D^s(x)$ for $x \in A$. Then for all $\epsilon > 0$, there exists a T such that*

$$D\phi_t S(x) < \epsilon$$

for all $t > T$.

Proof: By Property 3.1.7, $D\phi_t S(x) \to 0$ as $t \to \infty$. Hence for all $x \in A$, there is a time $T_0(x)$ after which

$$D\phi_t S(x) < \frac{\epsilon}{\alpha}$$

where α is the non-growth constant for the stable vectors coming out of U. By returns to U, there is some $T(x) > T_0(x)$ such that $\phi_{T(x)}(x) \in U$. By continuity and openness of U, there is an open neighborhood of x, $O(x)$, such that

$$\phi_{T(x)}\left(O(x)\right) \subset U,$$

and

$$D\phi_{T(x)} S(y) < \frac{\epsilon}{\alpha},$$

for all $y \in O(x)$. By the non-growth assumption, we have $D\phi_t S(y) < \epsilon$ for all $t \geq T(x)$. Now, the sets $O(x)$ form an open cover of A, and by passing to a finite subcover $O(x_1), \ldots, O(x_n)$, we can take $T = \max\{T(x_1), \ldots, T(x_n)\}$. Then by their selection, $D\phi_t S(y) < \epsilon$ for all $y \in A$ and $t > T$. $\Diamond$

We now integrate the distribution, and by a new trick, which we call the *book lemma*[2], show uniqueness. The name is derived from the nature of the proof. If there were multiple integrals, the weak-unstables would open like a book along the orbit of x, see Figure 3.2.1. We show that this violates basic properties of the flow.

One should note that the topological nature of this proof distinguishes it greatly from the more analytic nature of the typical Perron-type argument used in non-uniformly hyperbolic theory. The author believes that this could be useful in similar constructions because it allows conclusions that are topological in nature and hence not reliant on statistical behavior of orbits (often guaranteed by a pre-existing measure). However, this is at the expense of stronger conditions.

Proposition 3.2.2. *There exist C^1 unit speed curves of length ϵ, with derivatives lying in the unstable distribution centered at each point $x \in M_\epsilon$, that are unique up to orientation.*

Proof: Existence of the curves can be found by selecting an orientation for distribution in any contractible domain. From this orientation, we get a unit

[2]This name was suggested by O. Sarig during a talk in spring 2007.

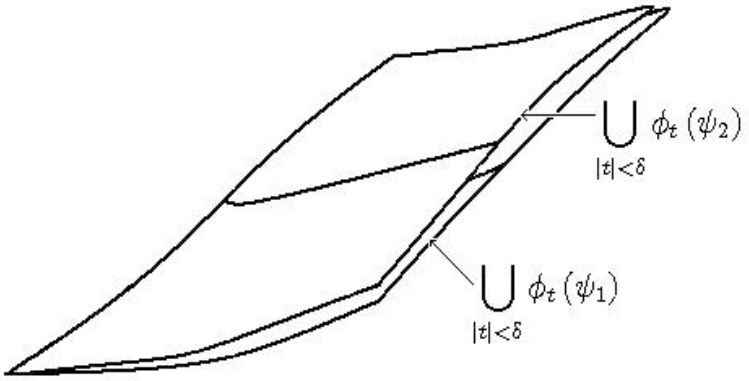

Figure 3.2.1. The generated weak-stables would open like a book.

length vector field at each point. This is a continuous vector field and hence there are integral curves. For ϵ sufficiently small, the ball of radius ϵ are contractible in M_0. Hence we have the integral curves of length at least ϵ.

The uniqueness of these curves (up to direction) can be seen in the following way. Assume there are two such curves ψ_1 and ψ_2. First, note that for $s \neq s'$ sufficiently small, $\phi_s(\psi_1)$ and $\phi_{s'}(\psi_2)$ have no intersection. If they did, then by the Lemma 3.2.1, $\phi_s(x)$ and $\phi_{s'}(x)$ would be asymptotic for negative time. This is impossible for $|s - s'|$ less than the length of the smallest periodic orbit.

Select $\delta > 0$ smaller than half the length of the smallest periodic orbit. Let y be a point in ψ_1 contained in boundary of the intersection of the weak-unstable manifolds given by $\bigcup_{|t|<\delta} \phi_t(\psi_i)$ for $i = 1, 2$. In a small enough neighborhood of y, we can consider the set of points between the weak-unstable manifolds, given by these two curves, and the unit length vector field of the unstable distribution.

All integral curves of any element z, between the weak-unstable manifolds, must intersect at least one of the weak-unstable manifolds. This would imply that there is a small neighborhood between the two imbedded manifolds that, again

by the Lemma 3.2.1, become uniformly close to the image of $\phi_t\left(\bigcup_{|s|<\delta}\phi_s(x)\right)$ as $t \to -\infty$. This would violate Property 3.1.9, that the system has no attractive orbits. $\Diamond$

Let $x \in M_0$ and not on a weak unstable of the singular. Then from Property 3.1.5, x has a pre-image in $U_{\hat{\epsilon}} \subset M_{\hat{\epsilon}}$. From Property 3.1.3, we can pull an unstable curve of length at least $\dfrac{\widehat{\epsilon}}{C}$ from the pre-image. Before expanding on this more, let us explore the continuity of these manifolds.

Let $\mathcal{S}_\epsilon$ be the class of continuous functions from $\left[-\dfrac{\epsilon}{2}, \dfrac{\epsilon}{2}\right]$ into M, with the C^1 metric, d_{C^1}. Furthermore, let $\tilde{\mathcal{S}}_\epsilon = \mathcal{S}_\epsilon/\sim$, where $f \sim g$ if $f(s) = g(s)$, or $f(s) = g(-s)$ for all $s \in \left[-\dfrac{\epsilon}{2}, \dfrac{\epsilon}{2}\right]$. The metric we use for $[f], [g] \in \tilde{\mathcal{S}}_\epsilon$ is

$$d([f],[g]) = \min\left\{d_{C^1}(f,g), d_{C^1}(f,\tilde{g})\right\},$$

where $\tilde{g}(s) = g(-s)$. We consider the local unstable manifolds as a map γ^u_ϵ from M_ϵ into $\tilde{\mathcal{S}}_\epsilon$.

We also use $\gamma^u_\epsilon(x)$ to denote the selection of one of the two possible orientations. Normally, this occurs when we have selected a vector field through D^u in a contractible neighborhood. In this setting, $\gamma^u_\epsilon(x)(s)$ denotes the image in M after moving along in the direction of the orientation a distance of s. The orientation does not change the image of the map.

Proposition 3.2.3. *As a map, γ^u_ϵ is C^1 continuous on M_ϵ in the C^1 metric mod orientation.*

Proof: For the points $x \in M_\epsilon$, let the distribution be given by a unit length vector field around x. This vector field is uniformly continuous in a closed neighborhood of x (of size greater than $\dfrac{\epsilon}{2}$). Consider any sequence of points $x_n \in M_\epsilon$ converging to x. Orient $\gamma^u_\epsilon(x_n)$ to agree with the vector field. By C^0 compactness of unit speed C^1 curves, we can select a convergent subsequence in the C^0 topology. By the uniform continuity of the vector field, the derivatives converge uniformly as well. Hence, the subsequence converges to a unit speed C^1 curve centered at x integrating the vector field. By uniqueness, it is $\gamma^u_\epsilon(x)$. Therefore, γ^u_ϵ is continuous, in this C^1 sense, on M_ϵ. $\Diamond$

For the global unstable manifolds, consider the following construction built inductively. Let $\epsilon_0 > 0$ be such that M_{ϵ_0} is nonempty. For each point $x \in M_0$, define $\epsilon(x) = \min\{\epsilon_0, d(x, N)\}$, and let

$$\Gamma_0^u(x) = Im\left(\gamma^u_{\epsilon(x)}(x)\right).$$

Now inductively, let

$$\Gamma^u_{n+1}(x) = \Gamma^u_n(x) \bigcup Im\left(\gamma^u_{\epsilon(y_1)}(y_1)\right) \bigcup Im\left(\gamma^u_{\epsilon(y_2)}(y_2)\right),$$

where y_1 and y_2 are the endpoints of $\Gamma^u_n(x)$. Finally, let the *global unstable* be

$$\Gamma^u(x) = \bigcup_{n=0}^{\infty} \Gamma^u_n(x).$$

Without much work, it can be seen that the global unstable manifolds partition M_0. We do not often use the global unstable manifolds directly.

Let M^u_L be the set of points for which the global unstable extends length $\dfrac{L}{2}$ in both directions. That is for $x \in M^u_L$, there is a unit speed curve γ^u_L from $\left[-\dfrac{L}{2}, \dfrac{L}{2}\right]$ into M_0 such that $\gamma^u_L(0) = x$ and the image of γ^u_L is contained in $\Gamma^u(x)$. Similar to above, we can think of these L length embedded sub-manifolds as a map γ^u_L from M^u_L into the space of C^1 curves from $\left[-\dfrac{L}{2}, \dfrac{L}{2}\right]$ into M mod orientation.

Note $x \in M^u_{\frac{\hat{\epsilon}}{2C}}$ unless it lies on one of the weak-unstables of the singular set. Furthermore, it is clear that $M_\epsilon \subset M^u_\epsilon$.

The next result gives us the continuity of longer pieces of unstable manifolds.

Proposition 3.2.4. *M^u_L is open and γ^u_L is continuous on M^u_L in the C^1 metric mod orientation.*

Proof: Let $x \in M^u_L$ and $\lambda > 0$ be given. Define $2\epsilon > 0$ to be the distance between the image of $\gamma^u_L(x)$ and the singular set N, and $n = \left[\dfrac{L}{\epsilon}\right]$, the smallest integer greater than the fraction. Now use the continuity of γ^u_ϵ on M_ϵ and pick $\delta_n > 0$ to be such that if $d(x_1, x_2) < \delta_n$ for x_1, x_2 in M_ϵ then

$$d\left(\gamma^u_\epsilon(x_1), \gamma^u_\epsilon(x_2)\right) < \min\{\lambda, \epsilon\}$$

in the C^1 metric. Pick $\delta_i > 0$ inductively so that $d(x,t) < \delta_i$ implies

$$d\left(\gamma_\epsilon^u(x), \gamma_\epsilon^u(y)\right) < \min\left\{\delta_{i+1}, \epsilon, \lambda\right\},$$

for $i = n-1, \ldots, 1$.

We claim that if $d(x,y) < \delta = \min\left\{\epsilon, \delta_1, \lambda\right\}$, then y is in M_L and $d\left(\gamma_L(x), \gamma_L(y)\right) < \lambda$. To see this, tile $\gamma_L^u(x)$ with ϵ-length local unstable manifolds in a way similar to the construction of the global unstable manifolds. Start with $\gamma_\epsilon(x)$. Inductively use $\gamma_\epsilon(x_j^i)$, $j = 1, 2$ where x_j^i are the endpoints of the previous step and extend in each direction by $\dfrac{\epsilon}{2}$. It takes at most n steps to cover $\gamma_L^u(x)$.

Now, y is in M_ϵ by selection of δ. Start with $\gamma_\epsilon^u(y)$ and let y_j^1, $j = 1, 2$ be the endpoints of $\gamma_\epsilon^u(y)$. By the selection of the δ_1, we have $d\left(x_j^1, y_j^1\right) < \min\left\{\delta_2, \epsilon\right\}$. Inductively from step i, we use $\gamma_\epsilon^u(y_j^i)$ to increase the curve length by $\dfrac{\epsilon}{2}$ in each direction and, by the selection of the δ_i, we have $d\left(x_j^i, y_j^i\right) < \min\left\{\delta_{i+1}, \epsilon\right\}$, for $i = 1 \ldots n-1$.

Hence, we are able to get a curve of length at least L and, by the selection of the δ_i, the C^1 distance between is $d\left(\gamma_L^u(x), \gamma_L^u(y)\right) < \lambda$. This gives us that M_L^u is open and γ_L^u is continuous there. $\Diamond$

Now, we briefly discuss unstable manifolds of the singular set. For $y \in N$, select a contractible neighborhood of y in $cl\left(U\right)$. By Property 3.1.8, the distribution is continuous in this neighborhood. Consequently, we can find a continuous unit length vector field through the distribution. As we did before we can integrate this from y. This integral will be unique because of the dichotomy property, and because it cannot vary only in the weak-unstable leaf. It can be extended as above.

Lemma 3.2.2. *For all $x \in M$, either $x \in M_L^u$ or lies in the strong unstable of a $y \in N$ with induced distance less than or equal to $\dfrac{L}{2}$.*

Proof: If x is not an element of $\gamma^u(y)$ for some y then $x \in M^u_{\frac{\epsilon}{2C}}$ for some constant. This follows from the discussion after Proposition 3.2.2. This result follows from the construction of the global unstable leafs. $\Diamond$

Now we consolidate our notation and terminology. We call γ_L^u the *local unstables* or *local unstable manifolds*. We abuse notation in the sense that γ_L^u is used to denote the mod-orientation map, the map with an orientation selected, and the submanifold given as an image of the map. So for example, $\gamma_L^u(x)$ can denote

the image and, for $s \in \left[-\frac{L}{2}, \frac{L}{2}\right]$, $\gamma_L^u(x)(s)$ denotes one of two elements of M depending on orientation. Similarly, we define γ_L^s to be the *local stables* or *local stable manifolds*. We let M_L^s be the equivalent to M_L^u for the local stables. The same properties hold. Often to stress the difference between the unstables and the weak-unstables (to be defined next), we use the term *strong* as in *local strong unstables* or *local strong stable manifolds*.

If $x \in M_L^u$ and $T > 0$, we can construct $\gamma_{L,T}^{u0}(x)$ as a function from $\left[-\frac{L}{2}, \frac{L}{2}\right] \times [-T, T] \longrightarrow M$ (mod orientation in the first coordinate; the two orientations give the same image) given by

$$\gamma_{L,T}^{u0}(x)(s,t) = \phi_t\left(\gamma_L^u(x)(s)\right).$$

We call these the *local weak-unstables* or *local weak-unstable manifolds*. We use the same abuse of notation: $\gamma_{L,T}^{u0}$ represents the map mod orientation in the first coordinate, the map with an orientation selected, and the image of said map. One should note that since ϕ_t is C^1, the map is C^1 mod orientation on M_L^u. Furthermore, from Proposition 3.3.1 we get that the map is an embedding, as long as T is less than half the length of the shortest periodic orbit.

Finally for y in the singular set, we use the notation of $\gamma_L^u(y)$ to represent the one-sided integral of length $\frac{L}{2}$ with $\gamma_{L,T}^{u0}(y)$, $\gamma_L^s(y)$, and $\gamma_{L,T}^{s0}(y)$ defined similarly.

3.3 Some Properties of Unstable Manifolds

We establish some properties of the unstable and stable manifolds away from the singular set. Most of these results are used in Section 3.5. The lone exception is Corollary 3.3.3, which is used in other chapters.

The first two properties demonstrate that the global unstable manifolds are immersed.

Lemma 3.3.1. *In M_ϵ, the local unstable manifold, γ_ϵ^u, cannot have an arbitrarily close intersection with itself.*

Proof: The proof works similarly to the proof for a minimal length closed orbit for flows on a compact manifold without fixed points using continuity of the local

unstable manifold. $\Diamond$

Proposition 3.3.1. *A global unstable manifold, Γ^u, cannot intersect itself.*

Proof: Let γ^u be a compact piece of an unstable manifold. By Lemma 3.2.1, we can find a $T > 0$, where for $t > T$, we have $l\left(\phi_{-t}\left(\gamma^u\right)\right) < \epsilon$. Since the local unstable curves do not intersect for the points in N and, by the dichotomy property, the rest always return to $U_{\hat{\epsilon}}$, we can conclude the result from the previous lemma. $\Diamond$

The next corollary gives us some continuity of the induced distance. It follows from the previous proposition, compactness of M_ϵ, and the continuity of local unstables. We let d_M denote the distance in the manifold and d_{γ^u} denote the induced distance within the unstable manifolds.

Corollary 3.3.1. *For any $\epsilon_1, \epsilon_2 > 0$ (ϵ_1 sufficiently small), there exists a $\delta = \delta\left(\epsilon_1, \epsilon_2\right) > 0$, such that if $x, y \in \gamma^u_{\epsilon_1}(z)$, with $z \in M_{\epsilon_1}$, satisfy $d_M(x, y) < \delta$, then $d_{\gamma^u}(x, y) < \epsilon_2$.*

Proof: Assume the contrary. Then for some given $\epsilon_1, \epsilon_2 > 0$, we would have a sequence of pairs of points (x_n, y_n) in local unstable manifolds in which the distance in the manifold goes to zero, but the induced distance is greater than or equal to ϵ_2. Let $c_n \in M_{\epsilon_1}$ be the center of the local stable manifolds. For each c_n select an orientation for $\gamma^u_{\epsilon_1}(c_n)$. Then $\gamma^u_{\epsilon_1}(c_n)$ is an isometry $\left[-\frac{\epsilon_1}{2}, \frac{\epsilon_1}{2}\right]$ into M, with respect to the induced metric.

Let (x'_n, y'_n) be the pre-images in $\left[-\frac{\epsilon_1}{2}, \frac{\epsilon_1}{2}\right] \times \left[-\frac{\epsilon_1}{2}, \frac{\epsilon_1}{2}\right]$ of (x_n, y_n) under the map $\gamma^u_{\epsilon_1}(c_n)$. By compactness of the interval, we can find a convergent subsequence, which we still call (x'_n, y'_n), converging to (x', y'). Because of the isometry, the distance between x' and y' is greater than or equal to ϵ_2 in the interval.

Now by the compactness of M_{ϵ_1}, we can choose a subsequence of the c_n that converges to some c in M_{ϵ_1}. By continuity of the local stables, we have the subsequence $\gamma^u_{\epsilon_1}(c_n)$ converging to a form of the local unstable manifold for c. But since the distance between the x_n and y_n goes to zero, the image of x' and y' would be the same. This contradicts Proposition 3.3.1. $\Diamond$

The following lemma is derived from the fact that distributions are transversal. It says that local unstables and weak-stables cannot intersect each other more than once.

Lemma 3.3.2. *For all $\epsilon > 0$, there exists a $\delta > 0$ such that for all $x \in M_\epsilon$ and $s_1, s_2, t_0 < \delta$,*

$$\gamma^u_{s_1}(x) \bigcap \gamma^{s0}_{s_2,t_0}(x) = \{x\}.$$

Proof: We can pick a contractible neighborhood. In this neighborhood, the distributions can be given by unit length vector fields. By the transversal nature of the vector fields, they can intersect at most once. We just need δ to be small enough so that the neighborhood of length 2δ is contractible in M_0. $\Diamond$

Corollary 3.3.2. *For all $\epsilon > 0$, there exists a $\delta > 0$ such that for all $x \in M_\epsilon$ and $s_1, s_2, t_0 < \delta$,*

$$\gamma^{s0}_{s_2,t_0}\left(\gamma^u_{s_1}(x)(s)\right) \bigcap \gamma^{s0}_{s_2,t_0}\left(\gamma^u_{s_1}(x)(s')\right) = \emptyset$$

is the empty set for $s \neq s'$.

Proof: This follows from the lemma above and the uniqueness of the leafs. $\Diamond$

The next lemma effectively states that local leafs foliate a uniform sized ball away from the singular set. One could prove equivalent statement switching the roles of strong and weak leafs.

Lemma 3.3.3. *For all $\epsilon > 0$, $\epsilon' > 0$, and $0 < s_1, s_2, t_0 < \delta$ sufficiently small, there exists a $\delta_0(s_1, s_2, t_0) > 0$ such that for all $x \in M_\epsilon$ we have*

$$\gamma^{s0}_{s_2,t_0}(\gamma^u_{s_1+\epsilon'}(x)) \supset B_{\delta_0(s_1,s_2,t_0)}\left(\gamma^u_{s_1}(x)\right),$$

the ball about $\gamma^u_{s_1}(x)$ of radius δ_0.

Proof: If we consider that the image, $\gamma^u_{s_1}$, is a continuous map with respect to the Hausdorff distance, as is $\partial\gamma^{s0}_{s_2,t_0}\left(\gamma^u_{s_1+\epsilon'}\right)$. The distance from these two sets is precisely the ball about $\gamma^u_{s_1}$ contained in $\gamma^{s0}_{s_2,t_0}\left(\gamma^u_{s_1+\epsilon'}\right)$. The distance is continuous and by compactness there exists a minimum. $\Diamond$

The next corollary follows from the previous and the fact that asymptotic behavior is the same along strong stables. It is useful for technical reasons because it allows us to pull unstables anywhere we want.

Corollary 3.3.3. *Points with forward dense orbits are dense on unstables.*

Proof: By Lemma 3.2.1, if x has a forward dense orbit, then so do all y on the the weak-stable of x. Now, let γ^u be a curve in an unstable. Consider $\gamma^{s0}_{\delta_1,\delta_2}(\gamma^u)$ where $\delta_1, \delta_2 > 0$ are chosen sufficiently small. This contains an open set and hence there is a point with a forward dense orbit. $\Diamond$

3.4 Behavior Near the Singular Set

In this section, we explore the behavior of the unstable manifolds as they approach the singular set. These estimates are crucial for showing that, after long term stretching, unstable manifolds are dominated outside of a neighborhood of the singular set.

By locally selecting an orientation, we can consider *onesided* local unstable manifolds. These are the pieces of the local unstable that go in the direction of the orientation. The next lemma shows that these halves, in some sense, vary continuously from "U"-side into the singular set. This follows from the integration of vector fields and the properties of the flow around the singular set.

For Lemma 3.4.1 to Corollary 3.4.1 we assume that the local unstables and stables are of an arbitrary fixed size.

Lemma 3.4.1. *Let $y \in N$ then for $x \in cl(U)$ as $x \to y$ we have that one half of $\gamma^u_\delta(x)$ approaches $\gamma^u_\delta(y)$ in the C^1 topology.*

Proof: Select a contractible neighborhood of y in $cl\,(U)$. By Property 3.1.8, the distribution is continuous in this neighborhood. Select the orientation of the continuous unit length vector field through the the distribution that points into U on the boundary. By a similar argument to Proposition 3.2.3, we can get a C^0 limit that must converge in C^1 to some C^1 integral. The only points that remain close and are asymptotic to $\phi_t(y)$ as $t \to -\infty$ are on $\gamma^u_\delta(y)$. So the limit must be $\gamma^u_\delta(y)$. $\Diamond$

The next lemma is used in part to give us finiteness of the measure constructed in Chapter 6. It comes from the continuity given by the previous lemma.

Lemma 3.4.2. *For $x \in cl(U)$ close enough to $y \in N$, the local unstable of x intersects the local weak-stable of y precisely once, if x is in U_{in} or on the local weak-stable, and not at all otherwise.*

Proof: Since the local onesided unstable of x converges to that of y, for x in U_{in}, it must intersect at least once. The unstable vector along the local weak-stable of y can either point into U_{in} or U_{miss} but not both; both would imply that the unstable vector is tangent at some point. By the first part of the proof, we know that it must point into U_{miss}. $\Diamond$

Take a contractible neighborhood of y minus the local weak-unstable manifold of y. On this neighborhood, we have a well defined unit length vector of the unstable distribution by selecting orientation. The next lemma tells us that the vector field has to "bend" around the singular set outside of U. This gives us a similar property for the integral.

Lemma 3.4.3. *On this neighborhood, the unstable vector has reversed orientation as it approaches from the two sides of the local weak-unstable of y in U.*

Proof: Select x close to y in U_{in}. By Lemma 3.4.2, the local unstable of x intersects the local weak-stable of y. Act on the local unstable of x by $\phi_{p(y)}$, where $p(y)$ is the period of y. Eventually, $\phi_{nt(y)}(x)$ will be in U_{out}. However, the local unstable of $\phi_t(x)$ will still intersect the local weak-stable of y. Hence, the integrated unstable moves from U_{in} into U_{out}. This implies that the orientation of the unstable vector is reversed. $\Diamond$

Lemma 3.4.4. *As x approaches y outside $cl\,(U)$ the local unstable of x intersects U_{in} on one side and U_{out} on the other side. Furthermore, the length that rests outside of U goes to zero.*

Proof: This follows from Proposition 2.6.1. $\Diamond$

In the next two results, we put these properties together to give us a picture of the behavior of the local stables and unstables near the singular set. The first result tells us that local unstables "wrap" around the local stables of the singular set, see Figure 3.4.1. The second result shows that local weak-unstables and local stables intersect twice "around" the singular set.

Proposition 3.4.1. *As x approaches y, the local unstable of x approaches a double copy of the onesided local unstable of y from the opposite sides of the the local weak-unstable of y in the C^0 topology.*

Proof: This follows from Lemmas 3.4.1 and 3.4.4. $\Diamond$

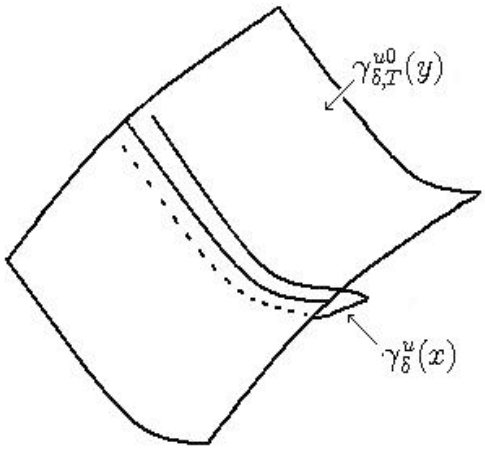

Figure 3.4.1. The local unstable approaches a double copy.

Corollary 3.4.1. *For x_1 and x_2 sufficiently close to $\in N$, the local stable of x_1 intersects the local weak-unstable of x_2 precisely twice; once in U_{miss} and once on the other side between the local weak-stable and unstable of $y \in N$.*

Proof: By adaptation of Lemma 3.4.2, we can cover a neighborhood of y by local weak-unstable manifolds identified by where they intersect the local stable of y. Since the distributions are transversal, they can intersect at most once in each region. By the fact that the local unstable and local stable converge to the local unstable and local stable (and hence weak do as well) respectively in both regions, they must intersect in each region at least once when they are sufficiently close. Since N is compact, the proximity necessary can be made uniform. $\Diamond$

The next corollary is what we use to "ignore" a neighborhood of the singular set. It effectively says that the percentage outside of a neighborhood can be made to dominate. It follows from the behavior of local unstables near the singular set.

Corollary 3.4.2. *There is an $L_0 > 0$ such that for every $\lambda > 0$, there exists an $\epsilon' > 0$, where the maximum length of a piece of unstable curve, between pieces of length at least L_0 in $M_{\epsilon'}$, has length less than λ.*

Proof: For $L_0 = \dfrac{\omega}{2}$ where ω is the guaranteed length of local one directional

unstables for elements of N. We can find an $\epsilon_0(y) > 0$ so that the length of the part of $\gamma_\omega(y)$ before exiting permanently an $\epsilon_0(y)$ neighborhood of N is less than $\frac{\lambda}{2}$.

From Lemma 3.4.1, we can choose $\epsilon_0(y) > \epsilon(y) > 0$ so that $d(x, y) < \epsilon(y)$ implies that the unstable has length at most λ before each side exits an $\epsilon_0(y)$ neighborhood of N. The $B_{\epsilon(y)}(y)$ form an open cover of N. By compactness of N, we can find a finite subcover with centers $y_1, \ldots, y_n$. There exists an $\epsilon' > 0$ so that x, in an $\epsilon' > 0$ neighborhood of N lies in $\epsilon(y_i)$, for some i in $1, \ldots, n$. $\Diamond$

3.5 Behavior Under Holonomy Maps

The core estimates of this chapter are presented here. We show that the holonomy maps do not change length and volume too much locally. These are the keys to the continuity of the strong-stable conditional measures and the holonomy invariance of the weak-unstable conditional measures.

For the following definitions, we assume that we have a local weak-unstable manifold $\gamma^{u0}_{L,T}$ and onesided stables coming out of it contained in a domain contractible in M_0. This implies that the stable and unstable distributions can be given as continuous unit length vector fields, and that everything is mapped injectively.

The *stable holonomy map* or *strong-stable holonomy map*, h_s, is defined between subsets of two local weak-unstables. If y lies on the local stable manifold of x, we say $h_s(x) = y$. The *time distance between two images*, $h_s(x_1)$ and $h_s(x_2)$, contained in the same local unstable $\gamma^{u0}_{L',T'}(z)$, is the difference $|t_1 - t_2|$ where $h_s(x_j) \in \phi_{t_j}(\gamma^u_{L'}(z))$ for $j = 1, 2$, see Figure 3.5.1. It is the time it takes to flow the local unstable of one into the local unstable of the other.

Similarly, the *weak-stable holonomy map*, h_{s0}, is defined between regions of two local unstable leafs. If y lies on the weak local stable manifold of x, we say $h_{s0}(x) = y$. We define the *time distance of the map* to be the maximum time distance between the weak-stable image of a point and the strong-stable image of the point in the same local unstable leaf.

The next three results deal with how these maps behave locally and uniformly for local unstables and local weak-unstables in the compact set M_ϵ. The first result

gives us the way that unstables are shifted under the map.

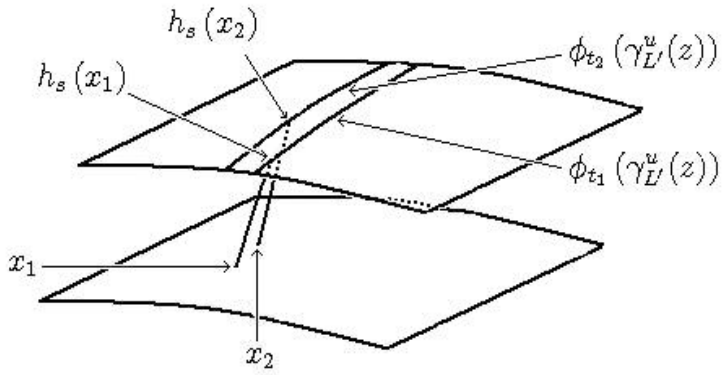

Figure 3.5.1. The time distance is $|t_1 - t_2|$.

Corollary 3.5.1. *For all $\epsilon > 0$, $\epsilon' > 0$, and $\epsilon > m(\epsilon) > m > 0$, there exists a $\tilde{\delta} = \tilde{\delta}(m, \epsilon') > 0$, such that for all $x \in M_\epsilon$ and $y \in M$ with $d(x, y) < \tilde{\delta}$, $\gamma^u_m(x)$ is weak-stable holonomy equivalent to a subset of $\gamma^u_{m+\epsilon'}(y)$ containing $\gamma^u_{m-\epsilon'}(y)$ with holonomy contained in $\gamma^{s0}_{\epsilon',\epsilon'}(\gamma^u_{m+\epsilon'}(y))$.*

Proof: Assume ϵ' is small. Let $m(\epsilon) > 0$ be chosen so that (i) all $y \in M_{\frac{\epsilon}{2}}$ are in $M^u_{m(\epsilon)+\epsilon'}$ and (ii) smaller than the δ for ϵ from Corollary 3.3.2. Let

$$\delta_1 = \frac{\delta(m + \epsilon', \epsilon')}{2} > 0,$$

where $\delta(m + \epsilon', \epsilon')$ is from Corollary 3.3.1. Let $\alpha = \min\{\epsilon', \delta_1\}$, and $\delta_0 = \delta_0(m + \epsilon', \alpha, \alpha) > 0$ be the value guaranteed as the contained neighborhood from the statement of Lemma 3.3.3. Choose $\frac{\epsilon}{2} > \tilde{\delta} > 0$ so that if $d(x, y) < \tilde{\delta}$ then the C^0-distance between $\gamma^u_{m+\epsilon'}(x)$ and $\gamma^u_{m+\epsilon'}(y)$ is less than $\min\{\alpha, \delta_1\}$.

For $x \in M_\epsilon$ and $d(x, y) < \tilde{\delta}$, we have

$$\gamma^u_m(x) \subset \gamma^{s0}_{\alpha,\alpha}\left(\gamma^u_{m+\epsilon'}(y)\right),$$

and hence $\gamma^u_m(x)$ is holonomy equivalent to a subset of $\gamma^u_{m+\epsilon'}(y)$. To see that it contains $\gamma^u_{m-\epsilon'}(y)$, consider $t \in [-m-\epsilon', m+\epsilon']$ where

$$\gamma^u_{m+\epsilon'}(y)(t) = h_{s0}\left(\gamma^u_m(x)(m)\right).$$

We have

$$\begin{aligned} d_M\left(\gamma^u_{m+\epsilon'}(y)(t), \gamma^u_{m+\epsilon'}(y)(m)\right) &\leq d_M\left(\gamma^u_{m+\epsilon'}(y)(t), \gamma^u_{m+\epsilon'}(x)(m)\right) \\ &\quad + d_M\left(\gamma^u_{m+\epsilon'}(x)(m), \gamma^u_{m+\epsilon'}(y)(m)\right), \\ &< 2\alpha \end{aligned}$$

and hence, by Corollary 3.3.1 and selection of α, $|t-m| < \epsilon'$ so $t > m - \epsilon'$. $\Diamond$

The next result is the strong-stable holonomy map equivalent to the previous result.

Corollary 3.5.2. *For all $\epsilon > 0$, $\epsilon' > 0$, and $m(\epsilon) > m > 0$, there exists a $\delta = \delta(m, \epsilon') > 0$ such that for all $x \in M_\epsilon$ the following holds: if $\gamma^{u0}_{m,t}(x)$ is stable holonomy equivalent to K with holonomy length less than δ and $y = h_s(x)$, then*

$$\gamma^{u0}_{m-\epsilon',t-\epsilon'}(y) \subset K \subset \gamma^{u0}_{m+\epsilon',t+\epsilon'}(y),$$

see Figure 3.5.2.

Proof: Let $\delta = \tilde{\delta}(m, \epsilon') > 0$ be as given in the Corollary 3.5.1. Furthermore, note that

$$K = \bigcup_{|r| \leq t} \phi_r\left(h_s\left(\gamma^u_m(x)\right)\right).$$

By selection of δ, $\gamma^u_m(x)$ is weak-stable holonomy equivalent to $\gamma^u_{m'}(y)$ with $m - \epsilon' \leq m' \leq m + \epsilon'$ and holonomy contained in $\gamma^{s0}_{\epsilon',\epsilon'}\left(\gamma^u_{m+\epsilon'}(y)\right)$. So,

$$\bigcup_{|q| \leq \epsilon'} \phi_q\left(h_s\left(\gamma^u_m(x)\right)\right) \supset \gamma^u_{m'}(y),$$

and therefore

$$\begin{aligned} K &= \bigcup_{|r|\le t} \phi_r\left(h_s\left(\gamma^u_m(x)\right)\right) \\ &= \bigcup_{|r|\le t-\epsilon'} \phi_r\left(\bigcup_{|q|\le \epsilon'} \phi_q\left(h_s\left(\gamma^u_m(x)\right)\right)\right) \\ &\supset \bigcup_{|r|\le t-\epsilon'} \phi_r\left(\gamma^u_{m'}(y)\right) \\ &= \gamma^{u0}_{m',t-\epsilon'}(y) \\ &\supset \gamma^{u0}_{m-\epsilon',t-\epsilon'}(y). \end{aligned}$$

Likewise,

$$\bigcup_{|q|\le \epsilon'} \phi_q\left(\gamma^u_{m'}(y)\right) \supset h_s\left(\gamma^u_m(x)\right)$$

gives us the other containment. $\Diamond$

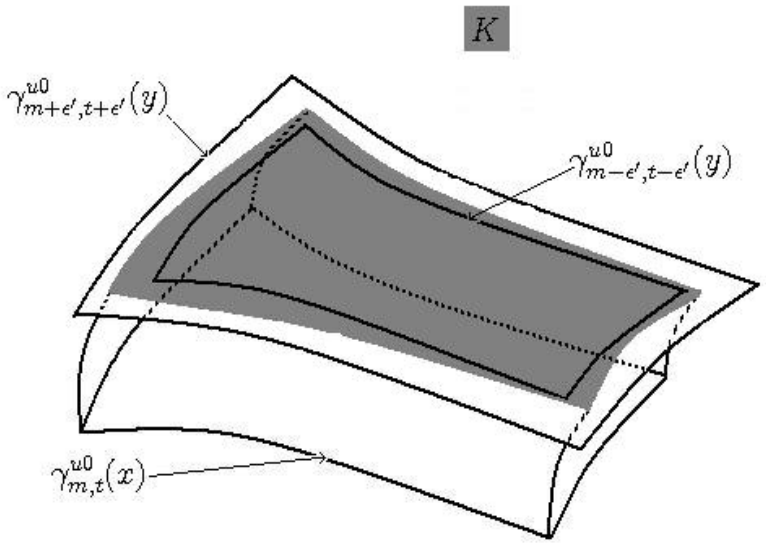

Figure 3.5.2. The holonomy image of a local weak-unstable.

We now turn the previous result into a statement on measure. We let *vol* denote the induced area of the weak-unstable leafs generated from the local stable maps. Note that since the unstable vector and the flow direction are orthogonal and the vector giving the flow is unit length, this is equivalent to integrating against length on the unstable followed by integrating against time.

Corollary 3.5.3. *For all $\epsilon > 0$, $\tilde{\epsilon} > 0$, and $m(\epsilon) > m > 0$, there exists a $\delta' = \delta'(m, s, \tilde{\epsilon}) > 0$ such that for all $x \in M_\epsilon$ the following holds: if $\gamma^{u0}_{m,t}(x)$ is stable holonomy equivalent to K with holonomy length less than δ', then*

$$\left|vol\left(K\right) - vol\left(\gamma^{u0}_{m,s}(x)\right)\right| \leq \tilde{\epsilon} vol\left(\gamma^{u0}_{m,s}(x)\right).$$

Proof: By the continuity of the volume, we can find a minimum volume, $C > 0$, for $\gamma^{u0}_{m,s}(x)$ where x varies over all of M_ϵ. Also, we can find $\epsilon' > 0$ so that for all $y \in M_{\frac{\epsilon}{2}}$, the difference in volume between $\gamma^{u0}_{m-\epsilon',s-\epsilon'}(y)$ and $\gamma^{u0}_{m+\epsilon',s+\epsilon'}(y)$ is less than $\dfrac{\tilde{\epsilon}C}{2}$. Furthermore, we can find a $\delta_0 > 0$ so that if $x, y \in M_{\frac{\epsilon}{2}}$, then the difference in volume between $\gamma^{u0}_{m,s}(x)$ and $\gamma^{u0}_{m,s}(y)$ is less than $\dfrac{\tilde{\epsilon}C}{2}$. Finally, we can use Corollary 3.5.2 to get the result. $\Diamond$

Chapter 4

Long Term Behavior on Unstable Manifolds

In this chapter, we take the structural results from Chapter 3 and turn them into dynamical consequences on long term behavior of the unstables. In the final section, we turn results on length into related results on integrals. The key results for the Margulis construction are Lemma 4.2.1, which gives holonomy invariance, Lemma 4.3.1, which gives compactness of a special class of linear functionals, and Lemma 4.3.2, which gives continuity of an operator on that class.

4.1 Comparative Growth Rate of Unstable Manifolds

We establish that the long term length of any two pieces of an unstable manifold is of the same order of magnitude. This is applied to obtain a similar result for integration of functions that are continuous with respect the induced topology of the unstables.

The first lemma is used in the proof of the corollary in this section and for technical reasons in Chapter 5. The basic idea of the proof is to interplay Corollary 3.4.2 and Corollary 3.5.1. The first corollary to say that we can ignore parts near the singular set and the second one to say that the behavior is good elsewhere.

Lemma 4.1.1. *Let γ_1^u and γ_2^u be unstable curves weak-stable holonomy equivalent*

with time distance less than s. Then for all $\tilde{\epsilon} > 0$, there exists a T_0 where $t \geq T_0$ implies

$$\frac{1}{\beta(s) + \tilde{\epsilon}} \leq \frac{l\left(\phi_t\left(\gamma_1^u\right)\right)}{l\left(\phi_t\left(\gamma_2^u\right)\right)} \leq \beta(s) + \tilde{\epsilon}.$$

Proof: Let $\tilde{\epsilon} > 0$ be given. Consider L_0 from Corollary 3.4.2 and let λ satisfy,

$$0 < \lambda < \frac{L_0 \tilde{\epsilon}}{3\left(\beta(s) + \tilde{\epsilon}\right)}.$$

Let $2\epsilon > 0$ be the ϵ' from the same corollary for λ. This is to say that the longest piece of unstable, between pieces of at least length L_0 contained entirely in $M_{2\epsilon}$, has length of at most λ.

Select $0 < m < m(\epsilon)$. By consequence of Corollary 3.5.1, we can select a $\delta > 0$ such that if $x \in M_\epsilon$ and $d(x, y) < \delta$, then $\gamma_m^u(x)$ is weak-stable holonomy equivalent to a subset of $\Gamma^u(y)$ with

$$l\left(\gamma_m^u(x)\right) < \left(1 + \frac{\tilde{\epsilon}}{3\beta(s)}\right) l\left(h_{s0}\left(\gamma_m^u(x)\right)\right). \quad \dagger$$

We can find a T_0 such that for all $t > T_0$,

$$l\left(\phi_t\left(\gamma_j^u\right)\right) > (n+2)L_0 + (n+2)\lambda, \quad \ddagger$$

where $n \in \mathbb{N}$ satisfies

$$nL_0 > \frac{6\left(\beta(s) + \tilde{\epsilon}\right)(m + \lambda)}{\tilde{\epsilon}}$$

for $j = 1, 2$. Furthermore, let T_0 be large enough that the stable distance of the holonomy is less than δ.

For $t > T_0$, we can do a maximal tiling of the part of $\phi_t\left(\gamma_1^u\right)$ in M_ϵ by tiles of length m starting from one end. Let $\widehat{\phi_t\left(\gamma_1^u\right)}$ represent the part of $\phi_t\left(\gamma_1^u\right)$ tiled and $\widehat{\phi_t\left(\gamma_2^u\right)}$ the subset of $\phi_t\left(\gamma_2^u\right)$ which is weak-stable holonomy equivalent to it. Any untiled part is either a tail end of length less than m, or lies in $B_{2\epsilon}(N)$, see Figure 4.1.1. By selection of δ, each tile is holonomy equivalent to a section of $\phi_t\left(\gamma_2^u\right)$ that is an s' time shift, with $|s'| < s$, of a piece of unstable of length that satisfies the inequality $\dagger$. Since the shift could at most shrink the sections by $\beta(s)$,

we have

$$\begin{aligned} l\left(\widehat{\phi_t\left(\gamma_1^u\right)}\right) &\leq \beta(s)\left(1+\frac{\tilde{\epsilon}}{3\beta(s)}\right) l\left(\widehat{\phi_t\left(\gamma_2^u\right)}\right) \\ &= \left(\beta(s)+\frac{\tilde{\epsilon}}{3}\right) l\left(\widehat{\phi_t\left(\gamma_2^u\right)}\right) \end{aligned} \quad . \S$$

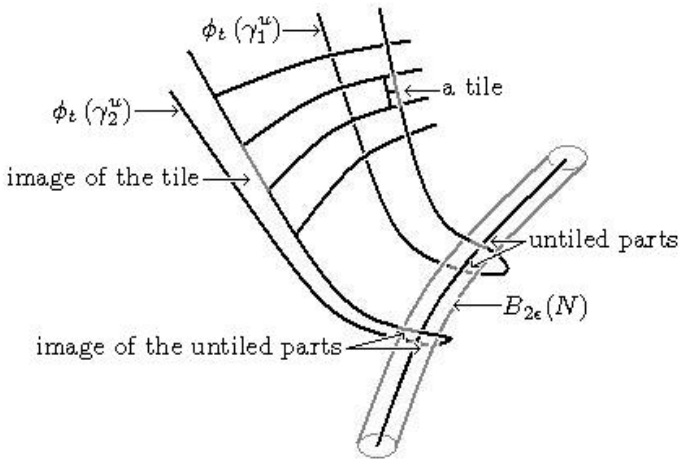

Figure 4.1.1. The tiling and its weak-stable image.

Now the untiled parts are contained in pieces of length less than λ and potentially a tail end of length less than m. Except for at most two of these pieces and the tail end, each of these pieces corresponds to a tiled section of length at least L_0. By ‡ and selection of λ, the total length, l_{total}, of these pieces satisfies

$$l_{\text{total}} < \frac{\tilde{\epsilon}}{3\left(\beta(s)+\tilde{\epsilon}\right)} l\left(\widehat{\phi_t\left(\gamma_1^u\right)}\right) . \ \sharp$$

Now the tiled part satisfies

$$l\left(\widehat{\phi_t\left(\gamma_1^u\right)}\right) > nL_0,$$

which, by the selection of n, implies that the remaining potential unaccounted for

parts length, $l_{\text{unaccounted}}$, satisfies

$$l_{\text{unaccounted}} < \frac{\tilde{\epsilon}}{3\left(\beta(s)+\tilde{\epsilon}\right)} l\left(\widehat{\phi_t\left(\gamma_1^u\right)}\right). \natural$$

By putting together §, ♯, and ♮,

$$\begin{aligned} l\left(\phi_t\left(\gamma_1^u\right)\right) &= l\left(\widehat{\phi_t\left(\gamma_1^u\right)}\right) + l_{\text{total}} + l_{\text{unaccounted}} \\ &\leq \left(1+2\frac{\tilde{\epsilon}}{3\left(\beta(s)+\tilde{\epsilon}\right)}\right)\left(\beta(s)+\frac{\tilde{\epsilon}}{3}\right) l\left(\widehat{\phi_t\left(\gamma_2^u\right)}\right) \\ &\leq \left(\beta(s)+\tilde{\epsilon}\right) l\left(\phi_t\left(\gamma_2^u\right)\right). \end{aligned}$$

The proof is finished by switching the roles of γ_1^u and γ_2^u in the estimations. ♢

The next result follows from the previous one and the density of forward dense orbits on unstables. It tells us that the long term growth of any two unstables is of the same order of magnitude and gives the compactness of a certain class of linear functionals presented in Chapter 5.

Corollary 4.1.1. *For any two nontrivial curves, γ_1^u and γ_2^u, contained in unstable manifolds, there exists a constant $A = A(\gamma_1^u, \gamma_2^u)$ such that*

$$\frac{l\left(\phi_t\left(\gamma_1\right)\right)}{A} \leq l\left(\phi_t\left(\gamma_2\right)\right) \leq A l\left(\phi_t\left(\gamma_1\right)\right)$$

for $t \geq 0$.

Proof: Use Corollary 3.5.1 and tile γ_1^u with unstables of length $m < m(\epsilon)$ where $\gamma_1^u \subset M_\epsilon$. Let n be the number of tiles and $x_1, \ldots, x_n$ be the center of these tiles. Let the tiles be given by ${}_i\gamma_1^u$. Take δ from the same corollary and some $\epsilon' >$. Let

$$B_i = B_\delta\left(x_i\right),$$

be the balls of radius δ, for $i = 1, \ldots n$. Pick a point y in the interior of γ_2^u with forward dense orbit and $\beta > 0$ such that $\gamma_\beta^u(y) \subset \gamma_2^u$. Let t_0 be such that for $t > t_0$,

$$\phi_t\left(\gamma_\beta^u(y)\right) \supset \gamma_{m(\epsilon)+\epsilon'}^u\left(\phi_t(y)\right).$$

Now by forward density, there are times $t_i > t_0$ such that $\phi_{t_i}(y) \in B_i$ for

$i = 1, \ldots, n$. Again by Corollary 3.5.1, the tile ${}_i\gamma_1^u$ is weak-stable holonomy equivalent to ${}_i\gamma_2^u$ a subset of $\gamma^u_{m(\epsilon)+\epsilon'}(\phi_{t_i}(y))$, which is itself a subset of $\phi_{t_i}(\gamma_2^u)$. By Lemma 4.1.1, there exists a C_i such that

$$\begin{aligned} l(\phi_t({}_i\gamma_1^u)) &\leq C_i l(\phi_t({}_i\gamma_2^u)) \\ &\leq C_i l(\phi_t(\phi_{t_i}(\gamma_2^u))) \\ &\leq \tilde{C}_i l(\phi_t(\gamma_2^u)), \end{aligned}$$

where $\tilde{C}_i$ is C_i times the maximum vector growth in time t_i. Let $C = \sum_{i=1}^{n} \tilde{C}_i$. Then for $t > \max\{t_i | i = 1, \ldots, n\}$, we have

$$\begin{aligned} l(\phi_t(\gamma_1^u)) &= \sum_{i=1}^{n} l(\phi_t({}_i\gamma_1^u)) \\ &\leq \sum_{i=1}^{n} \tilde{C}_i l(\phi_t(\gamma_2^u)) \\ &= C l(\phi_t(\gamma_2^u)). \end{aligned}$$

To get A just reverse the roles of γ_1^u and γ_2^u in the above argument and take the maximum. $\Diamond$

4.2 Long Term Behavior of Holonomy Equivalents

This is the result gives holonomy invariance and is therefore one of the core estimates. Similar to the way Corollary 3.4.2 and Corollary 3.5.1 are used in the proof of Lemma 4.1.1, here we interplay Corollary 3.4.2 and Corollary 3.5.3.

Lemma 4.2.1. *Let $\gamma^{u0}_{a,s}(x)$, with $0 < s \leq s_0$ and $a > 0$, be stable holonomy equivalent to K by holonomy h_s. Then for all $\epsilon' > 0$, there exists a T_0 such that for $t > T_0$ we have*

$$\left| \frac{vol(\phi_t(K))}{vol\left(\phi_t\left(\gamma^{u0}_{a,s}(x)\right)\right)} - 1 \right| \leq \epsilon'.$$

Proof: By Corollary 3.4.2, pick $\epsilon_1 > 0$ small so that the maximum length of a piece of an unstable curve, between pieces of the unstable curve of length at least L_0 contained in $M_{3\epsilon_1}$, is less than

$$\varepsilon = \frac{s\epsilon' L_0}{8\left(s+\frac{\epsilon_1}{2}\right)\beta^2\left(s+\frac{\epsilon_1}{2}\right)}.$$

By the same corollary, select $\epsilon_1 > 2\epsilon_2 > 0$ so that the maximum length of a piece of an unstable curve, between pieces of the unstable curve of length at least L_0 contained in $M_{2\epsilon_2}$, is less than ϵ_1. Select ρ so that if the induced unstable distance $d^u(y,y') < 2\rho$, then the time distance between $h_s(y)$ and $h_s(y')$ is less than $\frac{\epsilon_1}{2}$. Now cover $\gamma_a^u(x)$ with tiles of length less than or equal to ρ. Select T_0 so that if $t > T_0$, the following three conditions are met:

1. the length of all of the tiles is greater than ε,
2. $l\left(\phi_t\left(\gamma_a^u(x)\right)\right) > 2L_0$, and
3. the length of the stables is less than $\delta = \min\left\{\delta_1, \frac{\epsilon_1}{2}\right\}$ where $\delta_1 = \delta\left(m, s, \frac{\epsilon'}{2}\right)$ from Corollary 3.5.3 for $m = \min\left\{m(\epsilon_2), \epsilon_2\right\}$, where $m(\epsilon_2)$ comes from the same corollary.

Now let $t > T_0$ and consider

$$\left|vol\left(\phi_t\left(K\right)\right) - vol\left(\phi_t\left(\gamma_{a,s}^{u0}(x)\right)\right)\right|.\dagger$$

Tile as much of $\phi_t\left(\gamma_a^u(x)\right)$ as possible by tiles of the form $\gamma_m^u(x_j)$ starting from the ends where

$$x_j \in \phi_t\left(\gamma_a^u(x)\right) \cap M_{\epsilon_2},$$

$j = 1, \ldots, n$. This breaks † up into two parts. The first part is the sections that are contained in

$$\bigcup_{j=1}^{n} \gamma_{m,s}^{u0}\left(x_j\right).$$

To determine the first difference estimate let

$$K_j = h_s\left(\gamma_{m,s}^{u0}\left(x_j\right)\right) \subset \phi_t\left(K\right).$$

By the selection of δ and Corollary 3.5.3, we have

$$\left|vol\left(K_j\right) - vol\left(\gamma_{m,s}^{u0}\left(x_j\right)\right)\right| \leq \frac{\epsilon'}{2} vol\left(\gamma_{m,s}^{u0}\left(x_j\right)\right).$$

From this, we obtain

$$\left|\sum_{j=1}^{n}\left[vol\left(K_j\right) - vol\left(\gamma_{m,s}^{u0}\left(x_j\right)\right)\right]\right| \leq \frac{\epsilon'}{2} vol\left(\phi_t\left(\gamma_{a,s}^{u0}\left(x\right)\right)\right).\ddagger$$

Now we simply need to show that the remaining parts are small enough. There are two possibilities. Either $\phi_t\left(\gamma_a^u(x)\right)$ enters $B_{\epsilon_2}(N)$ or it does not. Since the case where it does not enter is simpler and uses the same basic argument, we only show it for the first case.

Since the tiling is maximal, the remaining part of the unstable leafs is at most ϵ_2 from being contained in the complement of M_{ϵ_2}. Let n' be the number of incidences where $\phi_t\left(\gamma_a^u(x)\right)$ enters the complement of $M_{2\epsilon_2}$ between sections of curve outside of length at least L_0 contained in $M_{2\epsilon_2}$. Call these pieces γ_j^u. Let y_j be the center of γ_j^u and $\tilde{\gamma}_j^u$ be the piece of $\gamma^u\left(\tilde{y}_j\right)$ weak-stable holonomy equivalent to γ_j^u where $\tilde{y}_j$ is the point stable holonomy equivalent to y_j, for $j = 1, \ldots, n$. Now the ends of γ_j^u must be in the complement of $M_{2\epsilon_2}$. By selection of ϵ_2,

$$l\left(\gamma_j^u\right) \leq \epsilon_1$$

and hence

$$\gamma_j^u \subset B_{2\epsilon_1}(N),$$

the ball of radius $2\epsilon_1$ about the singular set. By selection of t, pieces of the length of γ_j^u have both the time and stable distance of their weak-stable holonomy map less than $\frac{\epsilon_1}{2}$. Therefore,

$$\tilde{\gamma}_j^u \subset B_{3\epsilon_1}(N)$$

and hence it has length less than ε. So the remaining pieces of $\phi_t\left(\gamma_{a,s}^{u0}(x)\right)$ and $\phi_t\left(K\right)$ pieces are contained in

$$\bigcup_{j=1}^{n} \gamma_{\epsilon_1,s}^{u0}\left(y_j\right)$$

and

$$\bigcup_{j=1}^{n} \gamma^{u0}_{2\varepsilon, s+\frac{\epsilon_1}{2}}\left(\tilde{y}_j\right).$$

Since $\epsilon_1 < 2\varepsilon$, the difference in the volumes of the remaining pieces is not greater than

$$\sum_{j=1}^{n} \max\left\{vol\left(\gamma^{u0}_{2\varepsilon, s+\frac{\epsilon_1}{2}}\left(y_j\right)\right), vol\left(\gamma^{u0}_{2\varepsilon, s+\frac{\epsilon_1}{2}}\left(\tilde{y}_j\right)\right)\right\}.$$

Now by the definition of β, and taking crude estimates, this is less than

$$4n\left(s+\frac{\epsilon_1}{2}\right)\beta\left(s+\frac{\epsilon_1}{2}\right)\varepsilon = \frac{ns\epsilon' L_0}{2\beta\left(s+\frac{\epsilon_1}{2}\right)}.$$

Because there is a piece of $\phi_t\left(\gamma^u_a(x)\right)$ of length at least L_0 between γ^u_j and γ^u_{j+1}, the length satisfies

$$\begin{aligned} l\left(\phi_t\left(\gamma^u_a(x)\right)\right) &\geq \max\left\{(n-1)L_0, 2L_0\right\} \\ &\geq \frac{nL_0}{2}. \end{aligned}$$

Hence, we have the rough estimate that

$$\begin{aligned} vol\left(\phi_t\left(\gamma^{u0}_{a,s}(x)\right)\right) &\geq \frac{2sl\left(\phi_t\left(\gamma^u_a(x)\right)\right)}{\beta\left(s+\frac{\epsilon_1}{2}\right)} \\ &\geq \frac{snL_0}{\beta\left(s+\frac{\epsilon_1}{2}\right)}. \end{aligned}$$

The volume of the remaining pieces is less than

$$\frac{\epsilon'}{2} vol\left(\phi_t\left(\gamma^{u0}_{a,s}(x)\right)\right).$$

Putting this estimate together with estimate ‡,

$$\left|vol\left(\phi_t\left(K\right)\right) - vol\left(\phi_t\left(\gamma^{u0}_{a,s}(x)\right)\right)\right| \leq \epsilon' vol\left(\phi_t\left(\gamma^{u0}_{a,s}(x)\right)\right),$$

which is equivalent to the result. $\Diamond$

4.3 Translating to Functions

In order to undertake the Margulis construction, we translate the result of Section 4.1 into one relating to the integral of continuous functions. The remaining results are used to overcome technical difficulties.

Let T be the class of continuous compactly supported functions such that the function exists on one unstable leaf. Let ϕ_t act on T in the following way: $\phi_t(f) = f \circ \phi_t^{-1}$. Notice that the action simply permutes the class of functions. We start with the continuation of Lemma 4.1.1. This is used to show directly that the class of functionals is compact.

Lemma 4.3.1. *Let $f, f_0 \in T$ with f_0 a nonnegative nonzero function. There exists $C_1(f, f_0)$ such that*

$$\left| \frac{\int \phi_t(f)\, d\mu_u}{\int \phi_t(f_0)\, d\mu_u} \right| \leq C_1(f, f_0),$$

for all $t \leq 0$. Furthermore, if f is a nonnegative nonzero function, there exists $C_2(f, f_0)$ such that

$$\left| \frac{\int \phi_t(f)\, d\mu_u}{\int \phi_t(f_0)\, d\mu_u} \right| \geq C_2(f, f_0).$$

Proof: Let $K = supp(f)$ be the support of f in the leaf. By the assumption of compactness of the support, we know that $K \subset \gamma_2^u$ for some curve contained in the same leaf. Since f_0 is nonzero, we have some $\epsilon_0 > 0$ such that $f_0^{-1}([\epsilon_0, \infty)) \supset \gamma_1^u$ for some nontrivial curve contained in the support of f_0. By Corollary 4.1.1, there exists an $A = A(\gamma_1^u, \gamma_2^u)$ such that

$$\frac{l(\phi_t(\gamma_2^u))}{l(\phi_t(\gamma_1^u))} \leq A(\gamma_1^u, \gamma_2^u).$$

Then by the selections that we made, we have

$$\begin{aligned} \left| \frac{\int \phi_t(f)\, d\mu_u}{\int \phi_t(f_0)\, d\mu_u} \right| &\leq \frac{\|f_0\|_{\sup} l(\phi_t(\gamma_2^u))}{\epsilon_0 l(\phi_t(\gamma_1^u))} \\ &\leq \frac{\|f_0\|_{\sup} A}{\epsilon_0} \\ &=: C_1(f, f_0). \end{aligned}$$

For the other inequality, if f is nonnegative nonzero, we can reverse the roles of f and f_0 and use the first part to give the result. $\Diamond$

This next lemma gives continuity with respect to time of the actions of ϕ_t on the subset of the special linear functionals, as given in Section 5.1. It follows from Lemma 4.3.1 and uniform control of the growth of the differential.

Lemma 4.3.2. *Let $f, f_0 \in T$ both nonnegative nonzero functions. Then for every $\epsilon_0 > 0$, there exists a $t_0 > 0$ such that if $0 < t' < t_0$ then*

$$\left| \frac{\int \phi_{t+t'}(f)\, d\mu_u - \int \phi_t(f)\, d\mu_u}{\int \phi_t(f_0)\, d\mu_u} \right| \leq \epsilon_0$$

for all $t \geq 0$.

Proof: Since f is non-negative, we have

$$\frac{\int \phi_t(f)\, d\mu_u}{\beta(t_0)} \leq \int \phi_{t+t'}(f)\, d\mu_u \leq \beta(t_0) \int \phi_t(f)\, d\mu_u.$$

Since $\beta(t_0) \geq 1$,

$$\left| \int \phi_{t+t'}(f)\, d\mu_u - \int \phi_t(f)\, d\mu_u \right| \leq (\beta(t_0) - 1) \int \phi_t(f)\, d\mu_u.$$

By using $C_1 = C_1(f, f_0)$ from Lemma 4.3.1,

$$\left| \frac{\int \phi_{t+t'}(f)\, d\mu_u - \int \phi_t(f)\, d\mu_u}{\int \phi_t(f_0)\, d\mu_u} \right| \leq (\beta(t_0) - 1) C_1.$$

So picking $t_0 > 0$ small enough so that $\beta(t_0) \leq 1 + \dfrac{\epsilon_0}{C_1}$ gives the result. $\Diamond$

The remaining results tell us that the constant growth generated in Section 5.2 is not trivial, i.e. greater than one. We argue that there is a function whose integral has grown a uniform size under the action of our flow after a certain amount of time. We do this by selecting a periodic orbit and then arguing that its' local unstable, after enough time, must accumulate around the weak-unstable of the point. This accumulation allows us to dominate the integral of images of the function with longer term images.

Lemma 4.3.3. *Let γ^u be a curve of unstable and $x \in \gamma^u$ be a periodic point with*

period p. Then

$$l\left(\phi_{t+t'}\left(\gamma^u\right)\right) \geq \frac{l\left(\phi_t\left(\gamma^u\right)\right)}{\beta(p)},$$

for $t', t \geq 0$.

Proof: It follows from the fact that $\phi_{p+t}\left(\gamma^u\right) \supset \phi_t\left(\gamma^u\right)$ because the curves have to grow. So the minimum length can only occur for $0 \leq t \leq p$, which gives the estimate. $\Diamond$

Let $x \in M_\epsilon$ be a periodic point with period p. From Corollary 3.5.1, let $m = m(\epsilon)$. Select a continuous function f_1 on $\gamma^u(x)$ that satisfies the condition

$$\chi_{\gamma^u_{\frac{m}{2}}(x)} \leq f_1 \leq \chi_{\gamma^u_m(x)},$$

where χ represents the characteristic function of a set.

Lemma 4.3.4. *For all $D \geq 1$ and f_1 as above, there exists a $t_0 = t_0(D)$ such that*

$$\int \phi_{t+t'}\left(f_1\right) d\mu_u \geq D \int \phi_t\left(f_1\right) d\mu_u$$

for all $t \geq 0$ and $t' \geq t_0$.

Proof: Select any $\epsilon', \epsilon_0 > 0$, and n so that

$$\frac{n}{\beta(p)\left(\beta(\epsilon') + \epsilon_0\right)} \geq D.$$

Pick $x_1, \ldots, x_n$ distinct points with forward dense orbits in the interior of $\gamma^u_{\frac{m}{2}}(x)$. Pick $\mu > 0$ so that the $\gamma^u_\mu\left(x_j\right)$ are all disjoint. Use Corollary 3.5.1, the density of forward dense orbits, and the fact that the unstables grow, to select t_i so that $\gamma^u_m(x)$ is weak-stable holonomy equivalent to a subset of $\phi_{t_i}\left(\gamma^u_\mu\left(x_j\right)\right)$, with time distance less than ϵ'. By Lemma 4.1.1, there is a T_j such that $t > T_j$ implies that

$$\frac{1}{\beta(\epsilon') + \epsilon_0} \leq \frac{l\left(\phi_t\left(\phi_{t_j}\left(\gamma^u_\mu\left(x_j\right)\right)\right)\right)}{l\left(\phi_t\left(\gamma^u_m(x)\right)\right)}.$$

By Lemma 4.3.3, for all $t' \geq t_j + T_j$ and $t \geq 0$

$$l\left(\phi_{t+t'}\left(\gamma^u_\mu\left(x_j\right)\right)\right) \;=\; l\left(\phi_{t+t'-t_j}\phi_{t_j}\left(\left(\gamma^u_\mu\left(x_j\right)\right)\right)\right)$$

$$\begin{aligned} &\geq \frac{l\left(\phi_{t+t'-t_j}\left(\gamma_m^u(x)\right)\right)}{\beta(\epsilon')+\epsilon_0} \\ &\geq \frac{l\left(\phi_t\left(\gamma_m^u(x)\right)\right)}{\beta(p)\left(\beta(\epsilon')+\epsilon_0\right)}. \end{aligned}$$

Let $t_0 = \max_{i=1,\ldots,n}\{t_i + T_i\}$. Then for any $t \geq 0$ and $t' \geq t_0$,

$$\begin{aligned} \int \phi_{t+t'}\left(f_1\right) d\mu_u &\geq \sum_{j=1}^{n} l\left(\phi_{t+t'}\left(\gamma_\mu^u\left(x_j\right)\right)\right) \\ &\geq \sum_{j=1}^{n} \frac{l\left(\phi_t\left(\gamma_m^u(x)\right)\right)}{\beta(p)\left(\beta(\epsilon')+\epsilon_0\right)} \\ &\geq \frac{nl\left(\phi_t\left(\gamma_m^u(x)\right)\right)}{\beta(p)\left(\beta(\epsilon')+\epsilon_0\right)} \\ &= l\left(\phi_t\left(\gamma_m^u(x)\right)\right) \frac{n}{\beta(p)\left(C(\epsilon')+\epsilon_0\right)} \\ &\geq D\int \phi_t\left(f_1\right) d\mu_u, \end{aligned}$$

which is the desired result. $\Diamond$

Chapter 5

Construction of Conditional Measures

We adapt the arguments of G. Margulis from [Ma] to build conditional measures. The primary difference with that work is that the conditional measure is constructed directly on the unstable manifolds. Many of the properties require technically different proofs, but this chapter is subordinate to the spirit of that seminal work.

5.1 Special Linear Functionals

In this section, we examine a class of linear functionals that are of the form developed by G. Margulis for uniformly hyperbolic systems [Ma]. We define a couple of natural actions of the flow upon this class. These linear functionals live on the class of functions, T, presented in Section 4.3. This is the class of functions supported on a individual unstable leafs, which is continuous and compactly supported with respect to the induced topology of the leaf. This section follows fairly closely the work of G. Margulis. However, certain lemmas, which in statement are effectively the same, in particular Lemma 5.1.3, have proofs that differ significantly in form. This is due to technical differences that arise from the loss of uniform growth and the fact the construction here starts on the unstable manifolds directly.

Definition 5.1.1. *A family F of linear functionals on T satisfies the R-property*

if the following conditions hold:

R 1. *if for any $f \in T$, there exists a constant $c_1(f) > 0$ such that $|l(f)| \leq c_1(f)$ for any $l \in F$, and*

R 2. *if f is a nonnegative, nonzero function from T, then there exists a constant $c_2(f) > 0$ such that $l(f) \geq c_1(f)$ for any $l \in F$.*

We refine our sense of linearity to fit with our class of functions, T. The key difference from typical linearity is that T is not a vector space. Only if two functions are supported on the same leaf can they be added within the class.

Definition 5.1.2. *A functional h on T is called linear if*

1. *for any $f \in T$ and any real λ the equality $h(\lambda f) = \lambda h(f)$ holds, and*
2. *for any $f_1, f_2 \in T$ such that if $f_1 + f_2 \in T$, we have $h(f_1 + f_2) = h(f_1) + h(f_2)$.*

Define L as the space of functionals on T and T^* as the space of linear functionals. They are naturally real vector spaces and we use the topology of point-wise convergence on L; $\lim_{i\to\infty} h_i = h$, if $h_i(f) \to h(f)$ for every $f \in T$. This is the induced topology from viewing L as the infinite product $\Pi_{f\in T}\mathbb{R}_f$ with the Tychonoff topology, where the f coordinate of h is $h(f)$. Notice that L is locally convex. This is seen by considering the basis of the topology:

$$\left\{ \prod_{f\in T} I_f | I_f \text{ is an interval, and is } \mathbb{R} \text{ for all but a finite number of } F \right\}.$$

Clearly, T^* is a closed subset with respect to this topology. As a subspace of a locally convex vector space, $T^\star$ is locally convex. Furthermore, $K \subset L$ is compact if and only if K is closed and $\{h(f) | h \in K\}$ is a bounded subset of $\mathbb{R}$ for all $f \in T$.

The following three lemmas and propositions are effectively the same as in [Ma]. They expand on consequences of the topology. The proofs are all obvious.

Lemma 5.1.1. *If $F \subset L$ satisfies the R-property, then F is relatively compact in L.*

Proposition 5.1.1. *If F satisfies the R-property, then its closure, $\overline{F}$, also satisfies the R-property.*

Proposition 5.1.2. *If F satisfies the R-property, then the convex hull of F also satisfies the R-property.*

We now set up the subset of linear functionals that we are interested in. They are the ones generated by normalizing the pullback of length. The normalization is what gives compactness of the subset, an essential element of the Margulis construction.

Select $f_0 \in T$ non-negative, non-zero function. Let $T_1^* \subset T^*$ be the set

$$T_1^* = \{l_t : t \geq 0\},$$

where l_t is given by the following formula:

$$l_t(f) := \frac{\int \phi_t(f)\, d\mu_u}{\int \phi_t(f_0)\, d\mu_u}.$$

Let

$$T_2^* = \left\{ l = \sum_{i=1}^{k} c_i l_{t_i} : k \in \mathbb{N},\ t_i \geq 0,\ 0 \leq c_i,\ \text{and}\ \sum_{i=1}^{k} c_i = 1 \right\},$$

the convex hull of T_1^*.

Lemma 5.1.2. *T_2^* satisfies the* **R***-property.*

Proof: T_1^* satisfies **R**-property by estimates from Lemma 4.3.1. The rest follows from the properties above. $\Diamond$

Corollary 5.1.1. *The closure of T_2^*, $\overline{T}_2^*$, is compact and convex.*

Proof: Compactness follows from Lemma 5.1.1 and the convexity follows from construction of T_2^*. $\Diamond$

In G. Margulis' original work, the growth of unstable vectors is uniform. The following proposition is used to compensate for the non-uniform growth in this setting. We use the end of Section 4.3 to find a function that has a time for which the growth is uniform throughout the class of functionals.

Proposition 5.1.3. *There is an $f_1 \in T$ and a t' such that for all $l \in \overline{T}_2^*$, the following estimate holds:*

$$l\left(\phi_{t'}\left(f_1\right)\right) \geq 2l\left(f_1\right) > 0.$$

Proof: Use the f_1 and $t' > t_0$ for $D = 2$ from Lemma 4.3.4. The estimate holds for T_1^* by selection. By the definition of T_2^* and the topology of L, the estimate holds for $\overline{T}_2^*$. $\Diamond$

Via the definition of the action of ϕ_t on T, we define two actions of ϕ_t on L. The first is un-normalized and the second is normalized with a nonzero, nonnegative function, f_0, in the class. By the topology on L and because ϕ_t acts by permutation on T, both actions are continuous for fixed t. The following lemma shows that the actions are continuous, in terms of t, when acting on elements of our selected subclass, $\overline{T}_2^*$. This is despite the fact that the first action will not respect the class.

The un-normalized action is

$$\tilde{\phi}_t(l)(f) := l\left(\phi_t(f)\right),$$

and the normalized action is

$$\tilde{\tilde{\phi}}_t(l)(f) := \frac{\tilde{\phi}_t(l)(f)}{\tilde{\phi}_t(l)(f_0)}.$$

One should notice immediately that $\tilde{\tilde{\phi}}_t : \overline{T}_2^* \circlearrowleft$ because it clearly maps T_2^* into itself and it is continuous.

As promised, the following lemma gives us continuity for the two actions in terms of time. The continuity of the un-normalized action gives the continuity of the normalized action. The proof uses the topology of L to reduce it to showing continuity on the functions individually and Lemma 4.3.2 to argue continuity for a fixed function.

Lemma 5.1.3. *For any $l \in \overline{T}_2^*$, the map of the half-line $[0;\infty)$ to $\overline{T}_2^*$ taking $t \in [0;\infty)$ to $\tilde{\tilde{\phi}}_t l$ is continuous.*

Proof: By the topology on L, we need to show that $\tilde{\tilde{\phi}}_t l(f)$ is continuous as a map from $\mathbb{R} \longmapsto \mathbb{R}$ for all $f \in T$. This is done by showing that $\tilde{\phi}_t l(f)$ is continuous

for all $f \in T$, with f non-negative.

By Lemma 4.3.2, for every $\delta > 0$ there is a $t_0 > 0$ such that $0 \leq t' < t_0$ implies that

$$\begin{aligned} \left|\tilde{\phi}_{t'} l_t(f) - l_t(f)\right| &= \left|\frac{\int \phi_{t+t'}(f)\, d\mu_u - \int \phi_t(f)\, d\mu_u}{\int \phi_t(f_0)\, d\mu_u}\right| \\ &\leq \delta, \end{aligned}$$

for all $t \geq 0$ and l_t as defined above. Since the estimate is uniform, it holds for all $l \in \overline{T}_2^*$ and hence the map is continuous at $t = 0$. To see that it is continuous for all t, we note that $\phi_t(f)$ is a non-negative function. To see that it is continuous for all $f \in T$, write $f = f_+ - f_-$ where f_+ and f_- are both in T and nonnegative. Then $\tilde{\phi}_t l(f) = \tilde{\phi}_t l(f_+) - \tilde{\phi}_t l(f_-)$ and hence it is continuous. Finally the continuity of $\tilde{\tilde{\phi}}_t l(f)$ comes from $\tilde{\tilde{\phi}}_t l(f) = \dfrac{\tilde{\phi}_t l(f)}{\tilde{\phi}_t l(f_0)}$ being a ratio of continuous functions. $\Diamond$

5.2 Finding Conditional Measure on Unstable Manifolds

Here, we find a linear functional that displays the desired property of uniform growth and build conditional measures from it. The finding of the linear functional follows closely the argument of G. Margulis.

Lemma 5.2.1. *There exists a linear functional $\tilde{l} \in \overline{T}_2^*$ and a constant $d_u > 1$ such that for any real t*

$$\tilde{\phi}^t \tilde{l} = d_u^t \tilde{l}.$$

Proof: The proof of the existence of $\tilde{l}$ is precisely the proof used by G. Margulis in [Ma]. However, due to its significance in the present work, we repeat it here. The only difference here is how we show that d_u is non-trivial (it is obvious in the uniform growth case).

$\overline{T}_2^*$ is a compact convex set. By Tychonoff theorem, which assures a fixed point for any continuous action on a compact convex subset of a locally convex vector space, the set U_n of fixed points of $\tilde{\tilde{\phi}}_{\frac{1}{2^n}}$ is nonempty, for any natural n. Obviously, if $n_1 > n_2$, then $U_{n_1} \subset U_{n_2}$. Since the transformation $\tilde{\tilde{\phi}}_t$ is continuous for fixed t, U_n is closed for any n. Hence, the sets U_n form a sequence of nested compact sets, so their intersection is nonempty. This implies that there is a functional $\tilde{l} \in \overline{T}_2^*$

such that $\tilde{\tilde{\phi}}_{\frac{1}{2^n}}\tilde{l} = \tilde{l}$ for any positive integer n. Therefore, $\tilde{\tilde{\phi}}_{m\left(\frac{1}{2^n}\right)}\tilde{l} = \tilde{l}$ for any natural n and m. As $m\left(\frac{1}{2^n}\right)$ are dense in $\mathbb{R}^+$, we see, using Lemma 5.1.3, that $\tilde{\tilde{\phi}}_t\tilde{l} = \tilde{l}$ for any $t \geq 0$. Then, it is evident that $\tilde{\tilde{\phi}}_t\tilde{l} = \tilde{l}$ for $t < 0$ as well. Since $\tilde{\tilde{\phi}}_t\tilde{l} = \dfrac{\tilde{\phi}_t\tilde{l}}{\tilde{\phi}_t\tilde{l}(f_0)}$, we have $\tilde{\phi}_t\tilde{l} = h(t)\tilde{l}$ where $h(t) = \tilde{\phi}_t\tilde{l}(f_0)$. By the group property of $\tilde{\phi}_t\tilde{l}$,

$$h(t_1 + t_2) = h(t_1) \cdot h(t_2).$$

On the other hand, as is shown in Lemma 5.1.3, $\tilde{\phi}_t\tilde{l}(f)$ is continuous with respect to t. Therefore $h(t)$ is continuous. It follows that there exists a constant d_u such that $h(t) = d_u^t$.

Now we need to prove that $d_u > 1$. By Proposition 5.1.3, there exists an $f_1 \in T$ and $t' > 0$ such that

$$\tilde{l}\left(\phi_{t'} f_1\right) \geq 2\tilde{l}(f) > 0$$

and hence

$$d_u^{t'}\tilde{l}(f) = \tilde{\phi}_{t'}\tilde{l}(f) \geq 2\tilde{l}(f) > 0,$$

which implies that $d_u > 1$. $\Diamond$

We now turn this linear functional into conditional measures on the unstable leafs.

Lemma 5.2.2. *There exists measures μ_u on the unstable leafs such that*

$$\int f d\mu_u = \tilde{l}(f)$$

for all continuous f with compact support on a single unstable leaf.

Proof: This follows from Riesz representation theorem. $\Diamond$

Next we construct measures, μ_{u0}, on the weak-unstable leafs from $d\mu_u$ and dt. For functions that are continuous with compact support on a single weak-unstable leaf, we take the integral against $d\mu_u$ followed by integrating against dt. Let λ_t represent the pullback of length after time t on each leaf. Let λ_{t0} be the measures, constructed in the same fashion as above, from $d\lambda_t$ and dt. Furthermore, let $\tilde{\lambda}_t$ and $\tilde{\lambda}_{t0}$ be the normalized measure by the function f_0. Notice that $\tilde{\lambda}_t$ is the class of measure on the unstable leafs that corresponds to l_t.

Lemma 5.2.3. *On each weak-unstable leaf, the measure μ_{u0} is the weak* limit of the measures $\sum_{j=1}^{n_i} c_{i,j} d\lambda_{t_{j,i}0}$, where $\sum_{j=1}^{n_i} c_{i,j} l_{t_{i,j}} \longrightarrow_{i\to\infty} \tilde{l}$.*

Proof: Let f be a continuous function with compact support on a leaf. It can be decomposed into a finite sum of continuous functions with support in $\gamma^{u0}_{L,T}(y)$ for some L, T, and y. So we show the convergence for functions of this form. By the selection, for each $t \in [-T, T]$, $f_t = f|_{\phi_t(\gamma^u_L(y))}$ is a continuous function. Hence,

$$\lim_{i\to\infty} \sum_{j=1}^{n_i} \int c_{i,j} f_t d\tilde{\lambda}_{t_{j,i}} = \int f_t d\mu_u$$

for every t. Now there is a constant C where

$$\sup_{i,t} \left\{ \sum_{j=1}^{n_i} \int c_{i,j} f_t d\tilde{\lambda}_{t_{j,i}}, \int f_t d\mu_u \right\} \leq C.$$

Define the following functions g_i and g on $[-T, T]$ by $g_i(t) := \sum_{j=1}^{n_i} \int c_{i,j} f_t d\tilde{\lambda}_{t_{j,i}}$ and $g(t) := \int f_t d\mu_u$ for $i = 1, 2, 3, \ldots$. Then $g_i \to$a.e. g and is bounded on a set of finite measure, hence the convergence is in fact L^1. Thus the measures converge in the weak* sense. $\Diamond$

We can use ϕ_{-t} in the place of ϕ_t and the stable manifolds in place of the unstable manifolds to get μ_s and $d_s > 1$. For an equivalent definition of $\tilde{\phi}_t$, $\tilde{\phi}_t(\mu_s) = d_s^{-t}\mu_s$. All of the properties shown in the next section for μ_u, also hold for μ_s.

5.3 Holonomy Invariance and Other Properties

We establish the properties of the conditional measures that allow us to construct the Margulis measure in the next chapter. One key to that construction is the holonomy invariance of the weak-unstable conditional measure. This is the tool that allows the measure to be consistently defined in different flow boxes. The proof uses the characterization of μ_{u0} as a weak* limit on each leaf and a mild

variation of the standard trick; only a countable number of open balls about a point can have boundaries with positive measures.

Lemma 5.3.1. *The measures μ_{u0} are strong stable holonomy invariant.*

Proof: We show that open sets of the form int $\left(\gamma^{u0}_{a,s=a}(x)\right)$ and their holonomy images int (K), which have boundaries of measure zero, have the same measure. We suppress the interior in the notation. For any given center x, at most countably many a can have nonzero measure of the boundary for either them or their image. Since sets of these forms generate the topology, this implies that the measure is holonomy invariant.

Now take $\gamma^{u0}_{a,s=a}(x)$ and its holonomy image under the stable holonomy h_s, K. Notice that if the boundary has measure zero then so do the images of the set under ϕ_t. By our estimate from Lemma 4.2.1, for any $\epsilon > 0$ there is a $t_0 > 0$ such that

$$\left| \frac{vol\left(\phi_{t+t_0}\left(K\right)\right)}{vol\left(\phi_{t+t_0}\left(\gamma^{u0}_{a,s}(x)\right)\right)} - 1 \right| \leq \epsilon$$

for any $t > 0$. Since they are normalized by the same value, this would imply that for all $t > 0$

$$\left| \frac{\tilde{\lambda}_{t0}\left(\phi_{t_0}\left(K\right)\right)}{\tilde{\lambda}_{t0}\left(\phi_{t_0}\left(\gamma^{u0}_{a,s}(x)\right)\right)} - 1 \right| \leq \epsilon.$$

As this equation holds uniformly, it also holds for convex combinations. Furthermore, the set was selected to have zero measure on the boundary; it holds for μ_{u0}. Now

$$\frac{\mu_{u0}\left(\phi_{t_0}\left(K\right)\right)}{\mu_{u0}\left(\phi_{t_0}\left(\gamma^{u0}_{a,s}(x)\right)\right)} = \frac{d^{t_0}_u \mu_{u0}\left(K\right)}{d^{t_0}_u \mu_{u0}\left(\gamma^{u0}_{a,s}\left(x\right)\right)} = \frac{\mu_{u0}\left(K\right)}{\mu_{u0}\left(\gamma^{u0}_{a,s}\left(x\right)\right)},$$

which gives that

$$\left| \frac{\mu_{u0}\left(K\right)}{\mu_{u0}\left(\gamma^{u0}_{a,s}\left(x\right)\right)} - 1 \right| \leq \epsilon.$$

Since ϵ was arbitrary, we have

$$\mu_{u0}\left(K\right) = \mu_{u0}\left(\gamma^{u0}_{a,s}\left(x\right)\right),$$

which finishes the proof. $\Diamond$

We use the next lemma for technical reasons. It is proved by using holonomy

invariance and uniform growth of the measure to argue that if there were atoms, the measure would accumulate.

Lemma 5.3.2. *There are no atoms for μ_u.*

Proof: Assume that $\mu_u(\{x\}) \neq 0$. By the dichotomy property, there are two possibilities:

1. x lies on $\gamma^s(y)$ for some $y \in N$,
2. $\phi_t(x)$ has unbounded returns to $M_{\hat{\epsilon}}$.

If the first, then $\phi_{t(y)}(x) \in \gamma^s(x)$ where $t(y)$ is the period of y. This implies that

$$\mu_{u0}\left(\bigcup_{0\leq s\leq t(y)} \phi_s\left(\left\{\phi_{t(y)}(x)\right\}\right)\right) = \mu_{u0}\left(\bigcup_{0\leq s\leq t(y)} \phi_s\left(\{x\}\right)\right)$$

by holonomy invariance. However, by the growth property of μ_u,

$$\mu_{u0}\left(\bigcup_{0\leq s\leq t(y)} \phi_s\left(\left\{\phi_{t(y)}(x)\right\}\right)\right) = d_u^{t(y)}\mu_{u0}\left(\bigcup_{0\leq s\leq t(y)} \phi_s\left(\{x\}\right)\right),$$

a contradiction.

If the second, then there is some box centered in $M_{\hat{\epsilon}}$ of the form $\gamma^s_{s_2}\left(\gamma^{u0}_{s_1,t_0}(y)\right)$ for which $\phi_t(x)$ has unbounded returns. By holonomy invariance and growth of the measure, this would imply that $\gamma^{u0}_{s_1,t_0}(y)$ has infinite measure, a contradiction. $\Diamond$

The next lemma is the weak-unstable equivalent of strong-stable holonomy invariance. It gives us continuity of the strong stable conditional measures under small weak-stable holonomy.

Lemma 5.3.3. *If K_1^u and K_2^u are Borel sets in unstable manifolds weak-stable holonomy equivalent with time distance less than s, then*

$$\frac{1}{\beta(s)} \leq \frac{\mu_u(K_1^u)}{\mu_u(K_2^u)} \leq \beta(s).$$

Proof: It uses Lemmas 5.3.2 and 4.1.1 and works like Lemma 5.3.1. $\Diamond$

We define a *flow box* in the following way

$$B = \bigcup_{y \in \gamma^{u0}_{L,s}(x)} \gamma^s_y =: \gamma^s_y \left(\gamma^{u0}_{L,s}(x)\right),$$

where γ^s_y is given by picking another local weak-unstable leaf close to that of x and letting them cut the local stable for each $y \in \gamma^{u0}_{L,s}(x)$, see Figure 5.3.1. Select orientation so that γ^s_y can be viewed as a map from $[0, \tilde{s}(y)]$ into M.

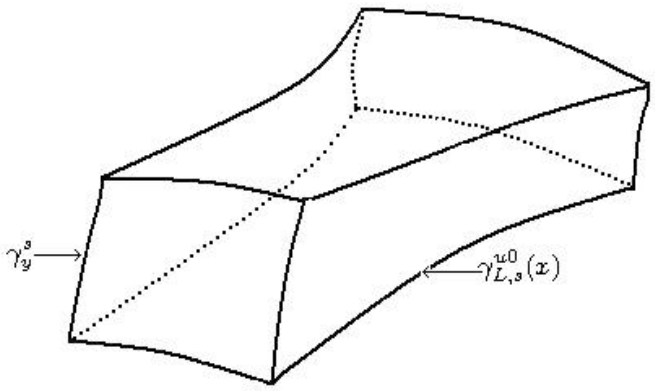

Figure 5.3.1. A flow box.

Let f be a continuous function on M with support contained in some flow box of the form above and let $f_{s,t} : [0, s'(y)] \to \mathbb{R}$ be given by

$$f_{s,t}(a) := f\left(\gamma^s_y\left(\gamma^{u0}_{s_1,t_0}(x)\,(s,t)\right)(a)\right).$$

Corollary 5.3.1. *With f given as above, then the function*

$$F(s,t) = \int_{\gamma^s_y} f_{s,t} d\mu_s$$

is continuous.

Proof: It follows immediately from Lemma 5.3.3 and the fact that compactly supported functions are uniformly continuous. $\Diamond$

In the next lemma, we use the uniform growth (or decay in negative time) to argue that the local weak-unstables of the singular set have finite measure. This is important because we build the measure on M_0, an open set, and hence cannot use compactness to guarantee finiteness.

Lemma 5.3.4. *For $y \in N$ then*

$$\bigcup_{t=0}^{p(y)} \phi_t\left(\gamma_\epsilon^u(y)\right),$$

where $p(y)$ is the period of y, has finite μ_{u0} measure.

Proof: We have $\bigcup_{t=0}^{p(y)} \phi_t\left(\gamma_\epsilon^u(y)\right) = \bigcup_{n=0}^{\infty} \phi_{-np(y)}\left(\bigcup_{t=0}^{p(y)} \phi_t\left(\gamma\right)\right)$ where γ is the piece of unstable between $\gamma_\epsilon^u(y)(\epsilon)$ and $\phi_{-p(y)}\left(\gamma_\epsilon^u(y)(\epsilon)\right)$. Let $D = d_u^{-p(y)} < 1$, then

$$\mu_{u0}\left(\phi_{-np(y)}\left(\bigcup_{t=0}^{p(y)} \phi_t\left(\gamma\right)\right)\right) = D^n \mu_{u0}\left(\bigcup_{t=0}^{p(y)} \phi_t\left(\gamma\right)\right)$$

and hence

$$\mu_{u0}\left(\bigcup_{t=0}^{p(y)} \phi_t\left(\gamma_\epsilon^u(y)\right)\right) = \sum_{n=0}^{\infty} D^n \left(\bigcup_{t=0}^{p(y)} \phi_t\left(\gamma\right)\right) < \infty,$$

because $D < 1$. $\Diamond$

Similarly and for the same purpose, we show that the local strong-stables of all the elements in the local weak-unstables of the singular set have bounded conditional measure.

Lemma 5.3.5. *For $\epsilon > 0$ sufficiently small, $\mu_s\left(\gamma_\epsilon^s(x)\right)$ is bounded for all $x \in \gamma_{\epsilon,p(y)}^{u0}(y)$ and $y \in N$.*

Proof: For ϵ sufficiently small, by adaptation of Lemma 3.4.2 and Corollary 3.4.1, $\gamma_\epsilon^s(x) \setminus \{x\}$ has two parts weak-unstable equivalent to a subset $\gamma_\delta^s(y)$ with time distance less than $p(y)$. Lemma 5.3.2 and Lemma 5.3.3 imply that the

measure is less than $2\beta\left(p(y)\right)$ that of $\gamma_{\delta}^{s}(y)$, which is bounded by adaptation of the proof of Lemma 5.3.4. $\Diamond$

Chapter 6

Construction of Margulis Measure

In this chapter, we construct a Margulis measure on M_0 that is invariant under the flow. We show that the measure is ergodic. These are used in the next chapter to get our main estimate.

6.1 From Flow Box to the Manifold

In keeping with the construction by G. Margulis, we first construct a measure in flow boxes then push it to the space M_0. We get invariance in the same fashion by showing the measure is finite. However, unlike in the uniform case, we cannot simply use compactness to argue finiteness. We instead use Lemmas 5.3.4 and 5.3.5.

For a flow box as in Section 5.3, construct a positive linear functional on continuous functions f with support contained in the interior by

$$I_B(f) = \int_{\gamma^{u0}_{s_1,t_0}(x)} \int_{\gamma^s_y} f\left(\gamma^s_y\left(\gamma^{u0}_{s_1,t_0}(x)\left(\tilde{s_1},t\right)\right)\left(\tilde{s_2}\right)\right) d\mu_s\left(\tilde{s_2}\right) d\mu_{u0}\left(\tilde{s_1},t\right).$$

Lemma 6.1.1. *For every flow box B, there exists a measure μ_B such that $I_B(f) = \int f d\mu_B$. Furthermore, let A be a borel set that is contained in two boxes B_1 and B_2. Then*

$$\mu_{B_1}(A) = \mu_{B_2}(A).$$

Proof: The first part suffices to show that I_B is indeed a positive linear functional. By Lemma 5.3.1, it is well defined and clearly a continuous linear functional.

So, we can apply the Riesz representation theorem to obtain a measure in the box. For the second part, from Lemma 5.3.1, integral is the same for any function with support contained in the interior of both of the boxes. By the construction in the Riesz representation theorem, this implies that any open set contained in interior of two boxes would have the same measure and hence, by regularity, any borel set. $\Diamond$

Now ϕ_t moves flow boxes B into other flow boxes $\phi_t(B)$ of the same form. One should note that the center may shift along the unstable in time. The next lemma describes how the measure is moved from one flow box to another by the flow.

Lemma 6.1.2. *For a flow box B acted upon by ϕ_t, the measures relate as follows*

$$\phi_t^* \mu_{\phi_t(B)} = d_s^{-t} d_u^t \mu_B.$$

Proof: It suffices to show that for continuous f with support in B we have

$$\int f \circ \phi_t^{-1} d\mu_{\phi_t(B)} = d_s^{-t} d_u^t \int f d\mu_B.$$

From the construction of μ_B above and the definition of the measures on the leafs, it holds. $\Diamond$

Because the measures are the same in the intersection of flow boxes, we can construct a measure $\tilde{\mu}$ on the borel sets of M_0. We break any borel set up into components that are contained in flow boxes.

Theorem 6.1.1. *The measure $\tilde{\mu}$ on M_0 is finite and invariant under ϕ_t.*

Proof: Once it is finite, from Lemma 6.1.2, $\tilde{\mu}\left(\phi_t\left(A\right)\right) = d_s^{-t} d_u^t \tilde{\mu}\left(A\right)$ for any Borel set A. Applying that to M_0 implies that $d_u = d_s$ and hence that it is invariant.

To prove that it is finite, we break N up into its separate orbits given by $y_1, \ldots, y_n$. For each y_j, break the weak-unstable in M_0 into the pieces of the form as in Lemma 5.3.4

$$F_{k,j} = \phi_{-kp(y_j)} \left(\bigcup_{t=0}^{p(y_j)} \phi_t\left(\gamma\right) \right)$$

where γ is the piece of unstable between $\gamma_\epsilon^u(y_j)(\epsilon)$ and $\phi_{-p(y_j)}\left(\gamma_\epsilon^u(y_j)(\epsilon)\right)$. Let $B_{k,j}$ be the flow box obtained by attaching $\gamma_\epsilon^s(x)$ cut off between a fixed weak-unstable

for each x of $F_{k,j}$. The sum of the measures of these boxes is less than supremum of the values for $\mu_s\left(\gamma_\epsilon^s(x)\right)$ times the measure of $\bigcup_{t=0}^{p(y)} \phi_t\left(\gamma_\epsilon^u(y)\right)$, which is finite by Lemmas 5.3.4 and 5.3.5. The measure of the weak-stable is zero because μ_u has no atoms. By Lemma 3.4.2 and Proposition 3.4.1, these cover an open neighborhood of N. By compactness of the rest, the measure is finite. $\Diamond$

We obtain via this proof a constant $k = d_u = d_s$. This constant is the one that gives the exponential growth in the main result. We let μ be the probability measure associated to $\tilde{\mu}$.

6.2 Properties of the Measure

In this section, we establish that the measure is ergodic. We use a standard Hopf-type argument. Namely, we argue that the forward and backward Birkhoff averages of continuous functions are constant on the weak-stable and weak-unstable leafs respectively. We then show that sets composed of these either have zero measure or positive measure of intersection.

Theorem 6.2.1. *The measure μ is ergodic.*

Proof: Because our space is a compact topological space and our measure Borel, we just need to show that the Birkhoff averages,

$$f_\tau^+ = \frac{1}{\tau}\int_0^\tau f\left(\phi_t(x)\right) dt,$$

converge to constants a.e. for f continuous, see [BS]. Let f^+ be the limit (that exists a.e.) and f^- be the the limit for ϕ_t^{-1}. Now $f^+ = f^-$ a.e. and by continuity of f, we have that f^+ is constant on weak-stables and that f^- is constant on weak-unstables. So, we complete the proof by showing that if A, A' are sets with positive measure that are unions of weak-stables and weak-unstables respectively, then $\mu\left(A \cap B\right) > 0$.

To do this first notice that A intersects some flow box with positive measure. Call this box B'. Now pick any other flow box, B. Pick t so that $\phi_{-t}\left(B'\right)$ has unstable length much smaller than the unstable length of B and intersects so that

the base of $\phi_{-t}(B')$ is holonomy equivalent to a subset of the base of B. This gives an intersection of positive measure with any flow box. Similarly, one can show intersection with positive measure of any flow box with A'.

Finally to see that A and A' have an intersection of positive, take any flow box, B. By adapting Lemma 5.3.3, A' intersects each stable leaf in B with positive measure bounded from below. This includes those contained in A. This gives positive measure of the intersection of A and A'. $\Diamond$

Chapter 7

Counting of Periodic Orbits

We continue to adapt the techniques used by G. Margulis in [Ma] to obtain the main result of the present work. We then briefly discuss the future of the research.

7.1 Finding Closed Orbits

Here, we show how to find closed orbits by looking at the way the flow acts on a flow box. This is a simplified version of the technique used by G. Margulis.

Pick $\epsilon > 0$ small and consider a flow box B (Section 5.3) of the form

$$\gamma_y^s \left(\gamma_{\epsilon, \frac{\epsilon}{2}}^{u0} (x) \right).$$

Let the cutting weak-unstable be chosen close enough so that the time shift between following an unstable then a stable versus following a stable and then an unstable, to arrive at the same orbit in B, is less than ϵ^2.

Now we consider B under the dynamics of the system, primarily the way $\phi_t(B)$ intersects B. It intersects between local weak-unstable leafs that intersect B. We consider *full components* of intersection to be a place where $\phi_t(B)$ intersects B, the unstables extend beyond the width of B, and they are contained between the weak-unstables defining the the top and bottom of B.

We show that each component of intersection contains a unique periodic orbit of time length between $t \pm \epsilon$.

Lemma 7.1.1. *Each full component of intersection of $\phi_t(B)$ and B contains a*

unique periodic orbit of period $t \pm \epsilon$, see Figure 7.1.1.

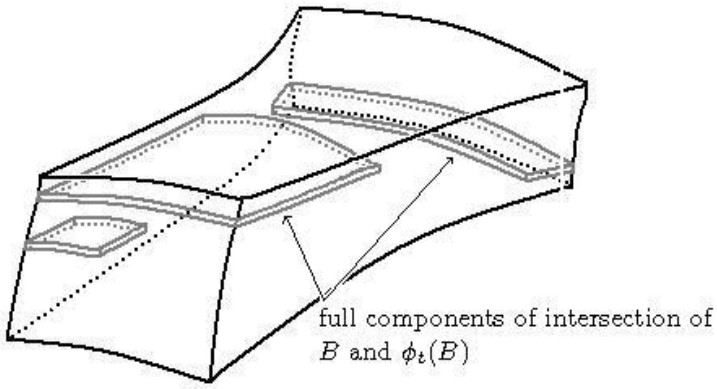

Figure 7.1.1. A closed orbit in each full component of intersection.

Proof: For each component, by a shift of at most ϵ, we can cause each weak-unstable leaf to intersect γ_x^s. From this, we can get a map from $\gamma_x^s \to \gamma_x^s$. Each z is mapped to the z' in γ_x^s where z' is the element of the weak-unstable of $\phi_t(z)$ in the component after the shift.

Taking images of γ_x^s under the iterates of the map, we get a nested sequence of compact sets. By taking intersection, we get an invariant set that clearly must be a single point. This point gives us a weak-unstable leaf that is mapped into itself by our shifted component. We can take a local unstable that runs across this leaf and reverse the process and get unique element of the unstable leaf. This corresponds to a periodic orbit of period not more than an ϵ shift of t. $\Diamond$

Our estimate on the number of periodic orbits rests on estimating the number of full components of intersection. We let

$$P_\epsilon(t) := \text{ number of periodic orbits of period } t \pm \epsilon.$$

We apply the previous lemma to find a relationship between the measure of the intersection and the number of periodic orbits.

Lemma 7.1.2. *Given $\epsilon > 0$, we have*

$$e^{-kt} t P_\epsilon(t) \geq C_1 \mu \left(\phi_t (B) \bigcap B \right) - C_2 e^{-kt},$$

for some $C_1, C_2 > 0$ constants and $t > t_0$.

Proof: By continuity of the strong-stable conditional measure, $0 < l_1 < \mu_s \left(\gamma_y^s \right) < l_2$. The measure of each component of intersection (in B) is therefore, by the exponential decay of μ_s, less than $e^{-kt} l_2 \mu_{uo} \left(\gamma^{u0}_{\epsilon, \frac{\epsilon}{2}}(x) \right)$. There are at most 4 components of intersection that are not full, the top and bottom of B, and the two sides of $\phi_t(B)$. Let $C(t)$ be the number of full components of intersection. We have

$$C(t) e^{-kt} l_2 \mu_{u0} \left(\gamma^{u0}_{\epsilon, \frac{\epsilon}{2}}(x) \right) + 4 e^{-kt} l_2 \mu_{u0} \left(\gamma^{u0}_{\epsilon, \frac{\epsilon}{2}}(x) \right) \geq \mu \left(\phi_t (B) \bigcap B \right).$$

By Lemma 7.1.1, this is nearly the estimate that we want. Now, we need to estimate how much we may have over counted. There is a minimum return time $\tilde{T} > 0$. So, the maximum number of times that a single periodic orbit could return is $\dfrac{t}{\tilde{T}}$. Simple manipulations give the result. $\Diamond$

7.2 Main Result

To obtain our estimate, we put together the technique from the previous section along with the property of ergodicity. Notice that k is the constant growth rate of the unstable conditional measure and does not depend on ϵ. However, the constant C in the statement does depend on ϵ.

Theorem 7.2.1. *There exists a $C = C(\epsilon) > 0$ such that for τ sufficiently large,*

$$\frac{1}{\tau} \int_0^\tau e^{-kt} t P_\epsilon(t) dt \geq C.$$

Proof: Integrating the left and right hand sides from Lemma 7.1.2, we get

$$\begin{aligned} \frac{1}{\tau} \int_0^\tau e^{-kt} t P_\epsilon(t) dt &\geq \frac{C_1}{\tau} \int_{t_0}^\tau \mu \left(\phi_t (B) \bigcap B \right) dt \\ &- \frac{C_2}{\tau} \int_{t_0}^\tau e^{-kt} \end{aligned}$$

$$\geq \overbrace{\frac{C_1}{\tau}\int_0^{\tau}\mu\left(\phi_t\left(B\right)\bigcap B\right)dt}^{\text{I}}$$
$$- \overbrace{\frac{1}{\tau}\left(C_1\int_0^{t_0}\mu\left(\phi_t\left(B\right)\bigcap B\right)dt+\frac{C_2}{k}\right)}^{\text{II}}.$$

Part I converges to $C_1\mu\left(B\right)^2 > 0$ by ergodicity, and part II converges to 0, which gives us the result. $\Diamond$

7.3 Further Work

The immediate future involves proving that the constant, k, is topological entropy. The author believes this can be accomplished through direct computation. One should then prove that the measure is mixing. The author hopes that a more sophisticated use of the *Hopf argument* will work. After that, one should try to apply this construction to similar systems.

Appendix A

Geometric Computations

A.1 Horizontal and Vertical Subspaces in Local Coordinates

Let M be a Riemannian manifold with the *Levi-Civita* connection. Let

$$\mathbf{x} : (x_1, \ldots, x_n) \in D \subset \mathbb{R}^n \to M$$

be a local patch with *Christoffel symbols* Γ_{ij}^k in these coordinates, for $i, j, k = 1 \ldots n$. Let X_i denote differentiation in the direction given by the coordinate i, $i = 1, \ldots n$. Parameterize locally the tangent bundle, TM, with $\mathbf{v} : (x_1, \ldots, x_n, y_1, \ldots, y_n) \in D \times \mathbb{R}^n \to TM$ given by

$$\mathbf{v}(x_1, \ldots, x_n, y_1, \ldots, y_n) = \sum_{i=1}^{n} y_i X_i \in T_{\mathbf{x}} M.$$

Let π and C_v be the projection map and the connection map as given in Section 1.5. In local coordinates, we want to develop $(d\pi_v, C_v) : T_v TM \to TM \bigoplus TM$. Let $\xi = \sum_{i=1}^{n} \tilde{x}_i X_i + \sum_{i=1}^{n} \tilde{y}_i Y_i \in T_v TM$. If v is given by $(x_1, \ldots x_n, y_1 \ldots y_n)$, then the most simple curve running through these points, with the proper derivative, is

$$\tilde{\gamma}(t) = (x_1 + t\tilde{x}_1, \ldots, x_n + t\tilde{x}_n, y_1 + t\tilde{y}_1, \ldots, y_n + t\tilde{y}_n).$$

Let $\gamma(t) = \pi \circ \tilde{\gamma}(t)$, which has

$$\left.\frac{d}{dt}\gamma(t)\right|_{t=0} = \sum_{i=1}^{n} \tilde{x}_i X_i.$$

For the connection map, the vector field is

$$V(t) = \sum_{i=1}^{n} \left(y_i + t\tilde{y}_i\right) X_i$$

varying over $\gamma(t)$. So,

$$\begin{aligned}
\left.\frac{D}{dt}V(t)\right|_{t=0} &= \sum_{i=1}^{n} \tilde{y}_i X_i + \sum_{i=1}^{n} y_i \nabla_{\left(\sum_{i=1}^{n} \tilde{x}_j X_j\right)} X_i \\
&= \sum_{i=1}^{n} \tilde{y}_i X_i + \sum_{i,j=1}^{n} y_i \tilde{x}_j \nabla_{X_j} X_i \\
&= \sum_{i=1}^{n} \tilde{y}_i X_i + \sum_{i,j,k=1}^{n} y_i \tilde{x}_j \Gamma_{ji}^{k} X_k \\
&= \sum_{k=1}^{n} \left(\tilde{y}_k + \sum_{i,j=1}^{n} y_i \tilde{x}_j \Gamma_{ji}^{k}\right) X_k.
\end{aligned}$$

From this, we can view $(d\pi_v, C_v) : \mathbb{R}^{2n} \to \mathbb{R}^n \times \mathbb{R}^n$ as the linear map where

$$\begin{gathered}
(d\pi_v, C_v)\left(\tilde{x}_1, \ldots, \tilde{x}_n, \tilde{y}_1, \ldots, \tilde{y}_n\right) = \\
\left(\left(\tilde{x}_1, \ldots, \tilde{x}_n\right), \left(\left(\tilde{y}_1 + \sum_{i,j=1}^{n} y_i \tilde{x}_j \Gamma_{ji}^{1}\right), \ldots, \left(\tilde{y}_n + \sum_{i,j=1}^{n} y_i \tilde{x}_j \Gamma_{ji}^{n}\right)\right)\right).
\end{gathered}$$

Immediately, we get the inverse map from $\mathbb{R}^n \times \mathbb{R}^n$ into $\mathbb{R}^{2n}$

$$\begin{gathered}
(d\pi_v, C_v)^{-1}\left(\left(\tilde{x}_1, \ldots, \tilde{x}_n\right), \left(\tilde{y}_1, \ldots, \tilde{y}_n\right)\right) = \\
\left(\tilde{x}_1, \ldots, \tilde{x}_n, \left(\tilde{y}_1 - \sum_{i,j=1}^{n} y_i \tilde{x}_j \Gamma_{ji}^{1}\right), \ldots, \left(\tilde{y}_n - \sum_{i,j=1}^{n} y_i \tilde{x}_j \Gamma_{ji}^{n}\right)\right).
\end{gathered}$$

The horizontal space, the pre-image of $\left(\left(\tilde{x}_1, \ldots, \tilde{x}_n\right), (0, \ldots, 0)\right)$, is the set

$$\left(\tilde{x}_1, \ldots, \tilde{x}_n, \left(-\sum_{i,j=1}^{n} y_i \tilde{x}_j \Gamma_{ji}^{1}\right), \ldots, \left(-\sum_{i,j=1}^{n} y_i \tilde{x}_j \Gamma_{ji}^{n}\right)\right),$$

and the vertical space, pre-image of $((0,\ldots,0),(\tilde{y}_1,\ldots,\tilde{y}_n))$, is the set

$$(0,\ldots,0,\tilde{y}_1,\ldots,\tilde{y}_n),$$

where $(\tilde{x}_1,\ldots,\tilde{x}_n)$ and $(\tilde{y}_1,\ldots,\tilde{y}_n)$ vary over $\mathbb{R}^n$.

A.2 Horizontal and Vertical Subspaces in Local Coordinates for the Unit Tangent Bundle of Surfaces

We examine the implications in the special case of a surface with an orthogonal parametrization. In particular, we are interested in formulas for the unit tangent bundle. For simplicity, we use the variables u, v, and notation for the metric $E = g_{11}$, $G = g_{22}$ and since by assumption it is orthogonal we have $F = g_{12} = g_{21} = 0$. Furthermore, we use the convention that subscripts mean differential with respect to the variable denoted, for example $E_u = \dfrac{\partial E}{\partial u}$. This gives us the Christoffel coefficients

$$\begin{aligned}
\Gamma^1_{11} &= \frac{E_u}{2E} \\
\Gamma^2_{11} &= -\frac{E_v}{2G} \\
\Gamma^1_{12} &= \frac{E_v}{2E} \\
\Gamma^2_{12} &= \frac{G_u}{2G} \\
\Gamma^1_{22} &= -\frac{G_u}{2E} \text{ and} \\
\Gamma^2_{22} &= \frac{G_v}{2G}.
\end{aligned}$$

Following immediately, we have a few more equalities that are not as profound, but that are used later:

$$\frac{\Gamma^1_{21}}{\sqrt{G}} = \left(\frac{E_v}{2\sqrt{G}\sqrt{E}}\right)\frac{1}{\sqrt{E}} \tag{A.1}$$

$$\frac{\Gamma^1_{22}}{\sqrt{G}} = \left(\frac{-G_u}{2\sqrt{G}\sqrt{E}}\right)\frac{1}{\sqrt{E}} \tag{A.2}$$

and

$$\frac{\Gamma^2_{11}}{\sqrt{E}} = \left(\frac{-E_v}{2\sqrt{G}\sqrt{E}}\right)\frac{1}{\sqrt{G}} \tag{A.3}$$

$$\frac{\Gamma^2_{12}}{\sqrt{E}} = \left(\frac{G_u}{2\sqrt{G}\sqrt{E}}\right)\frac{1}{\sqrt{G}}. \tag{A.4}$$

Because of the orthogonality, we can parameterize the unit tangent bundle by $\Psi : D \times S^1 \to D \times \mathbb{R}^2$ where (u, v, θ) is mapped to the unit vector given by $\frac{\cos\theta}{\sqrt{E}}\frac{\partial}{\partial u} + \frac{\sin\theta}{\sqrt{G}}\frac{\partial}{\partial v}$. By direct calculation, we have the following equations where $D\Psi$ is the differential of Ψ

$$\begin{aligned}
D\Psi\left(\frac{\partial}{\partial u}\right) &= X_1 - \left(\frac{E_u\cos\theta}{2E^{\frac{3}{2}}}\right)Y_1 - \left(\frac{G_u\sin\theta}{2G^{\frac{3}{2}}}\right)Y_2 \\
&= X_1 - \left(\frac{\Gamma^1_{11}\cos\theta}{\sqrt{E}}\right)Y_1 - \left(\frac{\Gamma^2_{12}\sin\theta}{\sqrt{G}}\right)Y_2 \\
D\Psi\left(\frac{\partial}{\partial v}\right) &= X_2 - \left(\frac{E_v\cos\theta}{2E^{\frac{3}{2}}}\right)Y_1 - \left(\frac{G_v\sin\theta}{2G^{\frac{3}{2}}}\right)Y_2 \\
&= X_2 - \left(\frac{\Gamma^1_{12}\cos\theta}{\sqrt{E}}\right)Y_1 - \left(\frac{\Gamma^2_{22}\sin\theta}{\sqrt{G}}\right)Y_2 \\
D\Psi\left(\frac{\partial}{\partial u}\right) &= -\left(\frac{\cos\theta}{\sqrt{E}}\right)Y_1 + \left(\frac{\sin\theta}{\sqrt{E}}\right)Y_2.
\end{aligned}$$

If we consider $(a, b, c, d) \in \mathbb{R}^4$ as the coefficients for the vectors X_1, X_2, Y_1, Y_2, respectively, in the tangent bundle TTM, then the span of $D\Psi$ is

$$\left(a, b, \frac{-\cos\theta\,(a\Gamma^1_{11} + b\Gamma^1_{12}) - c\sin\theta}{\sqrt{E}}, \frac{-\sin\theta\,(a\Gamma^2_{12} + b\Gamma^2_{22}) + c\cos\theta}{\sqrt{G}}\right),$$

where $(a, b, c) \in \mathbb{R}^3$ represent the coefficients of $\frac{\partial}{\partial u}, \frac{\partial}{\partial v}$, and $\frac{\partial}{\partial \theta}$ in TSM, respectively.

We determine the horizontal and vertical spaces for the tangent bundle of the unit tangent bundle. The projection is to those elements whose second coordinate

is orthogonal to the flow direction. In the local coordinates, it is the set,

$$(a,b)\bigoplus\left(\frac{-c\sin\theta}{\sqrt{E}},\frac{c\cos\theta}{\sqrt{G}}\right).$$

From Section A.1 and Equations A.1 to A.4, this has pre-image

$$\left(a,b,\tilde{c},\tilde{d}\right),$$

where

$$\begin{aligned}\tilde{c} &= \frac{-c\sin\theta}{\sqrt{E}}-\frac{a\cos\theta\Gamma^1_{11}}{\sqrt{E}}-\frac{b\cos\theta\Gamma^1_{12}}{\sqrt{E}}-\frac{a\sin\theta\Gamma^1_{21}}{\sqrt{G}}-\frac{b\sin\theta\Gamma^1_{22}}{\sqrt{G}}\\ &= \frac{-\cos\theta\left(a\Gamma^1_{11}+b\Gamma^1_{12}\right)-\sin\theta\left[\left(\frac{aE_v-bG_u}{2\sqrt{EG}}\right)+c\right]}{\sqrt{E}}\end{aligned}$$

and

$$\begin{aligned}\tilde{d} &= \frac{c\cos\theta}{\sqrt{G}}-\frac{a\cos\theta\Gamma^2_{11}}{\sqrt{E}}-\frac{b\cos\theta\Gamma^2_{12}}{\sqrt{E}}-\frac{a\sin\theta\Gamma^2_{21}}{\sqrt{G}}-\frac{b\sin\theta\Gamma^2_{22}}{\sqrt{G}}\\ &= \frac{-\sin\theta\left(a\Gamma^2_{12}+b\Gamma^2_{22}\right)+\cos\theta\left[\left(\frac{aE_v-bG_u}{2\sqrt{EG}}\right)+c\right]}{\sqrt{G}}.\end{aligned}$$

This has pre-image, in the tangent space for our coordinates of the unit tangent bundle, of

$$\left(a,b,\left(\frac{aE_v-bG_u}{2\sqrt{EG}}\right)+c\right).$$

So, the vertical space, generated by the unit vector $a,b=0$, and $c=1$, is

$$(0,0,1).$$

The horizontal space with the flow direction, generated by the unit vector $a=\frac{\cos\theta}{\sqrt{E}}$, $b=\frac{\sin\theta}{\sqrt{G}}$, and $c=0$, is

$$\left(\frac{\cos\theta}{\sqrt{E}},\frac{\sin\theta}{\sqrt{G}},\frac{\cos\theta E_v}{2E\sqrt{G}}-\frac{\sin\theta G_u}{2G\sqrt{E}}\right).$$

The horizontal space orthogonal to the flow, generated by the unit vector

$a = \dfrac{-\sin\theta}{\sqrt{E}}$, $b = \dfrac{\cos\theta}{\sqrt{G}}$, and $c = 0$, is

$$\left(\frac{-\sin\theta}{\sqrt{E}}, \frac{\cos\theta}{\sqrt{G}}, \frac{-\sin\theta E_v}{2E\sqrt{G}} - \frac{\cos\theta G_u}{2G\sqrt{E}}\right).$$

For the surfaces of revolution as given in Chapter 2, we have $E = f^2(v)$, $G = 1$ and hence $E_v = 2f'(v)f(v)$ and $E_v = G_u = G_v = 0$. Hence, the unit length vectors are $(0, 0, 1)$, $\left(\dfrac{\cos\theta}{f(v)}, \sin\theta, \dfrac{\cos\theta f'(v)}{f(v)}\right)$, and $\left(\dfrac{-\sin\theta}{f(v)}, \cos\theta, \dfrac{-\sin\theta f'(v)}{f(v)}\right)$, respectively.

A.3 The Differential on the Orthogonal Space for Geodesic Flows on Surfaces

From Section 1.5, we know that understanding the differential is related to understanding Jacobi fields. We restate the reduction of the Jacobi equation into a system of differential equations from [DC2] (p.110-112) and then apply it to surfaces. We have a setting just as in that section. That is, we have a Riemannian manifold $\tilde{M}$. Let n be the dimension.

Along a unit speed geodesic, $\gamma(t)$, we can consider parallel orthonormal frame $e_1(t), \ldots, e_n(t)$. Let $J(t)$ be a Jacobi field along $\gamma(t)$. Then we can decompose

$$J(t) = \sum_i f_i(t) e_i(t)$$

and let

$$a_{ij}(t) = \langle R\left(\gamma'(t), e_i(t)\right)\gamma'(t), e_j(t)\rangle$$

for $i, j = 1, \ldots n$. Then the Jacobi equation is equivalent to the following system

of differential equations

$$\begin{aligned} f_1''(t) + \sum_i a_{i1} f_i(t) &= 0 \\ &\vdots \\ f_n''(t) + \sum_i a_{in} f_i(t) &= 0. \end{aligned}$$

For the case where the manifold is a surface, let $e_1(t) = \gamma'(t)$. Then $e_2(t)$ is one of the two orthogonal normalized vectors. By the properties of the curvature tensor,

$$a_{11}(t) = a_{12}(t) = a_{21}(t) = 0.$$

Furthermore, since $e_2(t)$ is orthogonal and normalized,

$$a_{22}(t) = \kappa(t),$$

where $\kappa(t)$ is the curvature of the surface at that point. The system simplifies to

$$\begin{aligned} f_1''(t) &= 0 \\ f_2''(t) + \kappa(t) f_2(t) &= 0. \end{aligned}$$

If we consider elements of the orthogonal space, then we are only interested in solutions to the second equation.

Bibliography

[BP] Barreira, L.; Pesin, Y. *Lyapunov Exponents and Smooth Ergodic Theory*, American Mathematical Society, Providence, R.I., 2002.

[BDP] Boyce, W. E. and DiPrima, R. C., *Elementary Differential Equations*, vol. 2, Wiley, New York, 1969, 103-104.

[BS] Brin, M. and Stuck, G., *Introduction to Dynamical Systems*, Cambridge University Press, New York, 2002, 83-84.

[BG] Burns, K. and Gerber, M., *Real analytic Bernoulli geodesic flows on* S^2. Ergod. Th. & Dynam. Sys. 9 (1989), 27-45

[BK] Burns, K. and Katok, A., *Infinitesimal Lyapunov functions, invariant cone families and stochastic properties of smooth dynamical systems*, Erg. Theory and Dynam. Systems, 14 (1994), 757-785

[DC1] Do Carmo, M. P., *Differential Geometry of Curves and Surfaces*, Prentice-Hall, Upper Saddle River, New Jersey, 1976.

[DC2] Do Carmo, M. P., *Riemannian Geometry*, Birkhäuser, Boston, 1992.

[VD1] Donnay, V., *Geodesic flow on the two-sphere, Part I: Positive measure entropy*, Ergod. Th. & Dynam. Sys. 8 (1988), 531-553

[VD2] Donnay, V., *Geodesic flow on the two-sphere, Part II: Ergodicity, Dynamical Systems*, Springer Lecture Notes in Math., Vol. 1342 (1988), 112-153.

[Eb] Eberlein, P. *Geometry of Nonpositively Curved Manifolds*, University of Chicago Press, Chicago, 1996.

[Gu] Gunesch, R. *Precise Asymptotics for Periodic Orbits of the Geodesic Flow in Nonpositive Curvature*, Ph.D. Dissertation, Pennylvania State University, University Park, August 2002.

[HK] Hasselblatt, B. and Katok, A., *Introduction to the Modern Theory of Dynamics*, Cambridge University Press, New York, 1995.

[GK] Knieper, G. *Hyperbolic Dynamics and Riemannian Geometry*. Handbook of Dynamical Systems, Vol. 1A, Hasselblatt, B. and Katok, A., eds, Elsevier, Amsterdam 2002, 453-543

[Ma] Margulis, M. *On some Aspects of the Theory of Anosov Systems*, Springer, New York, 2004.

Vita

Bryce Weaver

PERSONAL DATA

BORN: September 7th 1975, Plymouth, Indiana

EDUCATION

PHD IN MATHEMATICS August 2008
Pennsylvania State University, University Park
Dissertation title: `Growth Rate of Periodic Orbits for Geodesic Flows on Surfaces with Regions of Positive Curvature`
Committee: Anatole Katok (Chair), Yakov Pesin, Omri Sarig, and David Abler

MASTER OF SCIENCE IN MATHEMATICS December 2001
University of North Carolina at Chapel Hill
Thesis title: `Extremal Distance and Capacity`
Committee: John Pfaltzgraff (Chair), Idris Assani, and Warren Wogan

BACHELOR OF SCIENCE IN MATHEMATICS, *summa cum laude* May 1998
Bridgewater College, Virginia
Minor: Chemistry